

STUDIES OF GEOMETRICAL ISOMERS BY
PHOTOIONIZATION MASS SPECTROMETRY

by

WILLIAM BRIEN STEWART
B.Sc., University of British Columbia, 1966

A THESIS SUBMITTED IN PARTIAL FULFILMENT OF
THE REQUIREMENTS FOR THE DEGREE OF
MASTER OF SCIENCE
IN THE DEPARTMENT
OF CHEMISTRY

We accept this thesis as conforming to the required standard

THE UNIVERSITY OF BRITISH COLUMBIA

September, 1968.

In presenting this thesis in partial fulfilment of the requirements for an advanced degree at the University of British Columbia, I agree that the Library shall make it freely available for reference and Study.

I further agree that permission for extensive copying of this thesis for scholarly purposes may be granted by the Head of my Department or by his representatives. It is understood that copying or publication of this thesis for financial gain shall not be allowed without my written permission.

Department of CHEMISTRY

The University of British Columbia
Vancouver 8, Canada

Date OCTOBER 25, 1968.

ABSTRACT

A series of isomeric tricyclic [3.2.1.0^{2,4}] oct-8-yl derivatives have been studied by photoionization mass spectrometry and the low resolution mass spectra of the compounds obtained. The observed differences in the relative intensities in the spectra of the isomers are explained on the basis of the geometry of the tricyclic system.

The major fragments of the low resolution spectra were 'mass measured' to determine their elemental composition and, from the information obtained, possible fragmentation pathways are postulated.

In addition, the ionization potential of all isomers was determined by electron impact.

TABLE OF CONTENTS

	<u>Page</u>
ABSTRACT	i
ACKNOWLEDGEMENT	v
I INTRODUCTION	1
II THEORETICAL	8
A. Photoionization and Dissociative Ionization	8
B. Ionization Potentials by Electron Impact	9
C. Operation of the Mass Spectrometer	13
III EXPERIMENTAL	16
A. Instrumental	16
B. Samples	22
C. Mass Spectra	25
D. Ionization Potentials	27
IV RESULTS AND DISCUSSION	29
A. Ketones	29
B. Methoxy Compounds	32
C. Hydrocarbons	34
D. Acetates	37
E. Alcohols	43
F. High Resolution	51
G. Ionization Potentials	58
V CONCLUSION	68
VI BIBLIOGRAPHY	70

LIST OF TABLES

	<u>Page</u>
I High Resolution Results for Tricyclic Ketones	52
II High Resolution Results for Saturated and Unsaturated Tricyclic Methoxy Compounds	53
III High Resolution Results for Tricyclic Hydrocarbons	54
IV High Resolution Results for Tricyclic Acetates	55
V High Resolution Results for Tricyclic Alcohols	56
VI High Resolution Results for Bicyclic Alcohols	57

LIST OF FIGURES

	<u>Page</u>
1. The Franck-Condon Principle	11
2. The M.S. 9 Mass Spectrometer	17
3. Dual Photon and Electron Impact Ion Source for M.S. 9	18
4. Photoionization Source	20
5. Compounds Studied	24
6. Mass Spectra of Tricyclic Ketones (a) Helium Light Source (b) Hydrogen Light Source	30
7. Mass Spectra of Tricyclic Methoxy Compounds (a) Helium Light Source (b) Hydrogen Light Source	33
8. Mass Spectra of Unsaturated Tricyclic Methoxy Compound (a) Helium Light Source (b) Hydrogen Light Source	35
9. Mass Spectra of Tricyclic Hydrocarbons (a) Helium Light Source (b) Hydrogen Light Source	36
10. Mass Spectra of Tricyclic Acetates, Helium Light Source	39
11. Mass Spectra of Tricyclic Acetates, Hydrogen Light Source	40
12. Mass Spectra of Tricyclic Alcohols, Helium Light Source	44
13. Mass Spectra of Tricyclic Alcohols, Hydrogen Light Source	45
14. Mass Spectra of Bicyclic Alcohols (a) Helium Light Source (b) Hydrogen Light Source	50
15. Fragmentation Scheme for Tricyclic Ketones	59
16. Fragmentation Scheme for Unsaturated Tricyclic Methoxy Compound	60
17. Fragmentation Scheme for Tricyclic Hydrocarbons	61
18. Fragmentation Scheme for Tricyclic Acetates	62
19. Fragmentation Scheme for Tricyclic Alcohols	63
20. Fragmentation Scheme for Bicyclo [2.2.1] heptan-7-ol	64
21. Fragmentation Scheme for <u>anti</u> -bicyclo [2.2.1] hepten-7-ol	65
22. Ionization Potentials for Compounds Studied.	67

ACKNOWLEDGEMENT

I wish to express my sincere gratitude to Dr. C.E. Brion for his continual help and guidance throughout the course of this work.

I would also like to thank Dr. D.C. Frost, Dr. G.R. Branton, Mr. G.E. Thomas, Mr. L.A.R. Olsen and Mr. J.S. Sandhu for their helpful discussions and assistance during the preparation of this thesis.

Special thanks are due to Dr. R.E. Pincock and Dr. J.S. Haywood-Farmer who generously provided the samples used in this study.

In addition, I would like to thank Mr. G.D. Gunn for his assistance in the operation of the mass spectrometer.

I INTRODUCTION

Little attention has been devoted to mass spectrometry with regard to the influence of stereochemistry on the fragmentation of organic molecules. Only two aspects have been demonstrated so far, namely the influence of the shape of the molecule which may be regarded as a crowding effect and the influence of the distance between interacting groups. For instance, Biemann (1) has discussed the difference in the behaviour of borneol and isoborneol on the basis of strain relief experienced by the molecular ion upon fragmentation. Elimination of water takes place to a greater extent in the more compact alcohol. Mandelbaum and Ginsberg (2) have shown that in some cases the fragmentation patterns of two epimers are dramatically different, where in a cyclic transition state a migration of one hydrogen is possible for only one of the isomers due to geometrical considerations. Gurst and Djerassi (3) have shown that androstane-2-one gives a very intense M-58 ion corresponding to the elimination of one molecule of acetone, possibly through a four membered transition state. Deuteration proves such a migration is impossible in the 10 α -epimer and this peak is not observed. In this example the distance factor is the effect which influences the fragmentation. It has been concluded (4) that if cases of hydrogen migration which can take place in one isomer only are ignored, the effect of stereochemistry on fragmentation in mass spectrometry is small, but there appears to be a correlation between stability in the thermodynamic sense and the ability for the compound to fragment upon electron impact.

The difference in structure between geometrical isomers is characterized by the relative spatial position of some atoms or groups in the molecule. The proximity of these atoms or groups, in a particular spatial configuration, can produce non-bonded interactions in the molecule, and a steric hindrance often exists in one isomer but not in the other (5). The study of geometrical isomers by mass spectrometry has been the subject of a number of investigations (1-14). The majority of these studies have been carried out utilizing a conventional electron impact ionization source and only very slight differences are observed in the mass spectra of two isomers of the same substance. The observed differences between the mass spectra of the two isomers have been found to depend on the energy of the ionizing electrons, being generally more pronounced at lower electron energies. Using electron impact mass spectrometry for the study of geometrical isomers Natalis (5) has found,

- (1) for the trans isomer, the relative abundance of the molecular ion is greater, than that of the cis isomer, especially for low electron energies.
- (2) the ionization potential is essentially the same for both isomers, however, the appearance potentials of the main fragment ions are lower for the cis isomer. This indicates that less energy is required to cause further decomposition of the ionized cis molecule.
- (3) the probability of decomposition of metastable ions is larger in the cis isomer than in the trans, for several processes.

Brion and Hall (18) have studied the cis and trans isomers of 4-t-butylcyclohexanol using a photoionization source (19, 20) in a mass spectrometer. They have observed significant differences in the mass spectra of the two isomers which have been attributed to steric factors. Previous studies of these compounds, by the same authors, using a conventional electron impact ion source gave results which were inconclusive and could not be reproduced. These results were attributed to spurious processes caused by the hot filament and the accompanying high temperature of the ion chamber. These high temperatures are one of the major disadvantages of electron impact ion sources, since compounds may undergo significant thermal decomposition. The use of photoionization eliminates many of the problems associated with conventional electron impact ion sources. Poschenrieder and Warneck (21) have shown that the lack of a filament also minimizes outgassing and memory effects. Another advantage is that the photon energy is precisely determined whereas in electron impact work there is not only a Maxwellian thermal spread of electron energies but also space charge and contact potentials which can modify the nominal energy. This is especially serious at low electron energies and can lead to lack of reproducibility in the mass spectra due to the difficulty of obtaining the same absolute electron energy. While it is true that fragmentation can be reduced if an electron impact source is operated at low energies, the resulting loss in sensitivity cannot usually be tolerated (22).

Photoionization spectra are also more amenable to comparison with theories of mass spectra since the energy of the ionizing radiation is closely defined.

Poschenrieder and Warneck have discussed the use of an ultraviolet monochromator as a convenient, narrow band energy selector. With energy selection applied in the mass spectrometric analysis of complex gas mixtures, a selective ionization of only a few of the involved components can be achieved (21) in contrast to the ionization of all the components as is customary with electron impact sources. Accordingly, the mass spectrum is simplified and the overlap and interference resulting from individual components can be minimized.

The earliest description of the use of a beam of photons to produce ionization was by Terenin and Popov (23). From the beginning the technique has developed until it is possible to measure the cross-sections for photoionization in gases at low pressures (24) and to measure the ionization potential of gases (25). Watanabe and co-workers (25) used a 1-meter normal incidence vacuum monochromator with a resolution of 1 \AA^0 .

However, photoionization sources for mass spectrometers received relatively little attention probably due to the technical difficulties involved in their operation. Interest in the technique was revived in 1956, when Lossing and Tanaka (26) described some preliminary experiments on the performance and characteristics of a photoionization source, used in conjunction with a mass spectrometer. Instead of a monochromator they used the direct ultraviolet light from a krypton discharge lamp which had been fitted with a lithium fluoride window. The

lithium fluoride window will only transmit wavelengths greater than 1050 \AA ($< 11.8 \text{ e.v.}$) and molecules with ionization potentials greater than this therefore cannot be studied.

Terenin and Villesov (27) and Morrison, Hurzeler and Inghram (28, 29) have used a combination of a vacuum monochromator and a mass spectrometer in detailed studies of the formation of ions by photon impact. The source of light was a high voltage hydrogen lamp with a lithium fluoride window to isolate the residual gases in the light source from the ionization chamber. If very efficient differential pumping is employed it is not necessary to isolate the light source from the high vacuum of the mass spectrometer with a lithium fluoride window. A windowless differentially pumped system places no restriction on the energy of the transmitted photon beam.

Weissler, Samson, Ogawa and Cook (30) and also Comes and Lessmann (31) were able to obtain results up to about 30 e.v. using a low pressure repetitive spark source and differential pumping. A simple windowless system for photoelectron spectroscopy has been used by Al-Joboury and Turner (32) and by Frost, McDowell and Vroom (33). Photoionization sources have been exploited in mass spectrometry by Frost, Mak and McDowell (34), by Dibeler and Reese (35) and by Berkowitz and Chupka (36). However, these instruments have been primarily designed for the study of threshold ionization phenomena. In this work grating monochromators are used to vary the wavelength in a precise manner. The resulting photon fluxes are very low due to the high resolving power and low reflectivity of the diffraction grating at the wavelengths used. Such a device is generally not suitable for the ionizing source of an analytical mass

spectrometer for which a high ionizing flux at a single and preferably high energy is usually required.

The choice of a light source for vacuum ultraviolet radiation depends on the particular application. Continuum sources are generally more desirable for providing information at all wavelengths, as for example in absorption studies. Continuous radiation can be produced both by the interaction of electrons with atoms or molecules and by the acceleration (synchrotron radiation) or deceleration (bremsstrahlung radiation) of free electrons.

Line radiation is often preferred for mass spectrometric studies. It is usually produced by electronic transitions between different energy levels in neutral atoms and molecules and in ions. Roman numerals placed after the symbols for the elements indicate whether the radiation is emitted from the neutral atom (I) or from ions of various degrees of ionization (II, III). Radiation produced by transitions between excited states and the ground state of the atom or ion is called resonance radiation.

The problem of producing radiation of a given wavelength (i.e. of a given energy) involves the formation of the appropriate excited atom or ion. In general, the shortest wavelengths (highest energy) are produced from the most highly ionized atoms. A dc glow discharge tends to produce radiation from neutral atoms whereas more energetic discharges such as the spark discharge are necessary to produce highly ionized atoms.

Line sources using undispersed radiation and suitable for use in a mass spectrometer have been described by Brion (19), Omura and Doi (37, 38, 39) and also Beynon and co-workers (40). In these studies

a microwave or dc discharge is used to produce either the $584.3 \text{ \AA}^{\circ}$ (21.21 e.v.) helium resonance line (He I) or the $1215.7 \text{ \AA}^{\circ}$ (10.19 e.v.) hydrogen Lyman-alpha line (H I). The results of photoelectron spectroscopy indicate the essential monochromaticity of these light sources.

The intensity of ions produced, in a particular state, by photons is usually a maximum at threshold and thereafter generally decreases with increasing photon energy (42) while for electron impact ionization the intensity of ions increases as a function of electron energy above threshold (41). Due to the nature of the photoionization threshold law the light sources used in this study provide sufficient energy to give satisfactory mass spectra.

II THEORETICAL

A. Photoionization and Dissociative Ionization

This work is concerned mainly with the ionizing collisions of photons with molecules. A molecule can absorb a photon of energy $h\nu$ exciting the system from a state of lower energy E'' to a state of higher energy E' , i.e.

$$h\nu = E' - E'' \quad 1.$$

where h is Planck's constant and ν is the frequency of the radiation.

Photoexcitation is the process of absorption of radiation by a molecule. It can be represented by



where xy and xy^* are ground and excited states of the molecule respectively.

Photoionization can occur by the interaction of a photon of sufficiently high energy with the molecule xy . The major processes resulting from the photoionization of molecules may be summarized as follows:

1. Simple Ionization



The minimum photon energy necessary for this process is called the adiabatic ionization potential of xy . Beyond the energy of the ionization threshold there is a region of continuous absorption for each quantum state.

2. Dissociative Ionization

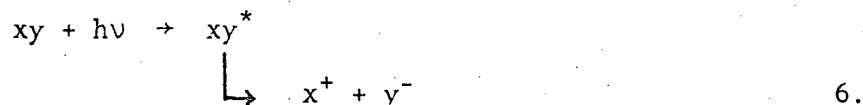


The minimum photon energy necessary for this process is called the appearance potential of x^+ . The dissociation energy or bond strength of the molecule $D(x-y)$ can be calculated from the appearance potential by the following relationship

$$V(x^+) = D(x - y) + I(x) + K.E. + E.E. \quad 5.$$

where $V(x^+)$ is the appearance potential of atom x , $I(x)$ is the ionization potential of x , $K.E.$ is the excess kinetic energy of the process and $E.E.$ is the excitation energy which ion or neutral fragment may possess. Most atomic ionization potentials are known from optical spectroscopy and provided that the $K.E.$ and $E.E.$ are known the dissociation energy can be obtained by measurement of the appearance potential.

3. Ion Pair Formation

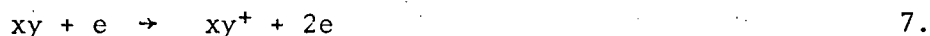


B. IONIZATION POTENTIALS BY ELECTRON IMPACT

An extensive study of the ionization potentials of a large number of atoms and molecules has been carried out by a large number of workers, for example see Field and Franklin (46). In addition to the

technique of electron impact the following methods of measuring ionization potentials have been employed: optical spectroscopy, photoelectron spectroscopy, theoretical and semi-empirical calculations, charge transfer and photon impact.

The ionization potential of an atom or molecule is theoretically defined (43) as the minimum amount of energy required to completely remove an electron from the neutral species in its ground state.



However, the ionization potentials measured may not correspond to this definition because the possibility exists that the product or products of the ionization process may be in a vibrationally excited state. Thus the ionization potential is generally defined in electron impact studies, as the minimum energy of the bombarding electrons at which the formation of 'parent' ions can be detected.

The Franck-Condon principle, first proposed by Franck (44) and later formulated mathematically by Condon states that, in an electronic transition, the nuclear separation and velocity of relative motion alter to a negligible extent i.e. the transition takes place so quickly that there is no change in the nuclear coordinates.

Figure 1 illustrates the application of the Franck-Condon principle to ionization phenomena for a diatomic molecule. The transitions are all taken as originating from the zeroth vibrational level of the initial electronic state. The maximum probability for transition occurs in the center of the Franck-Condon region.

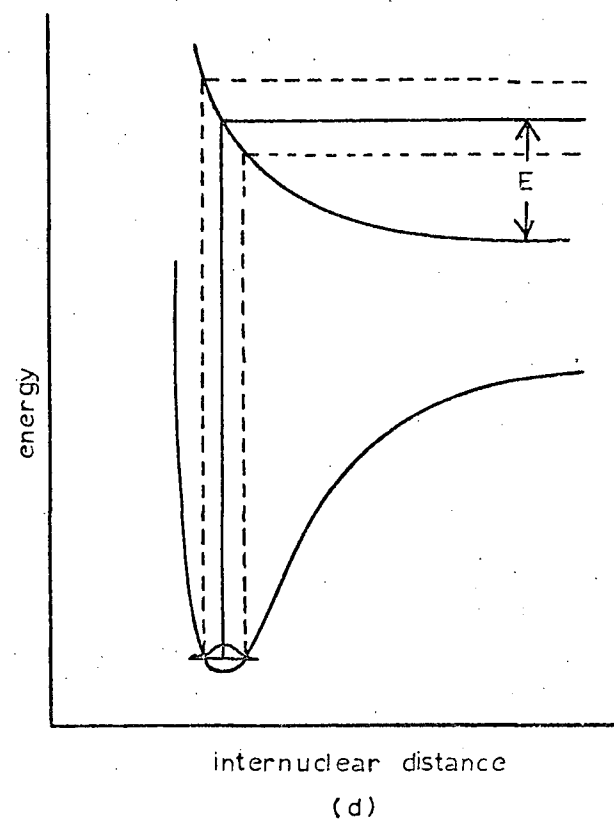
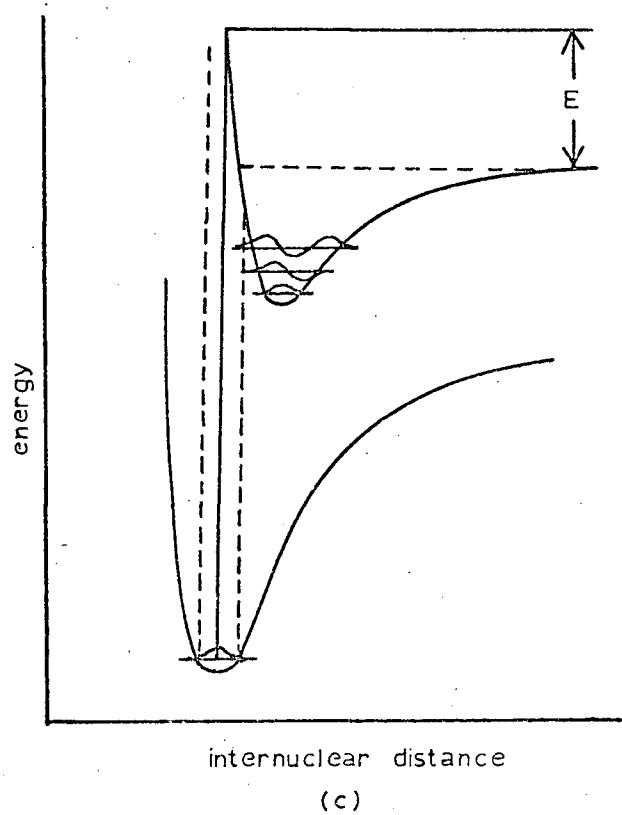
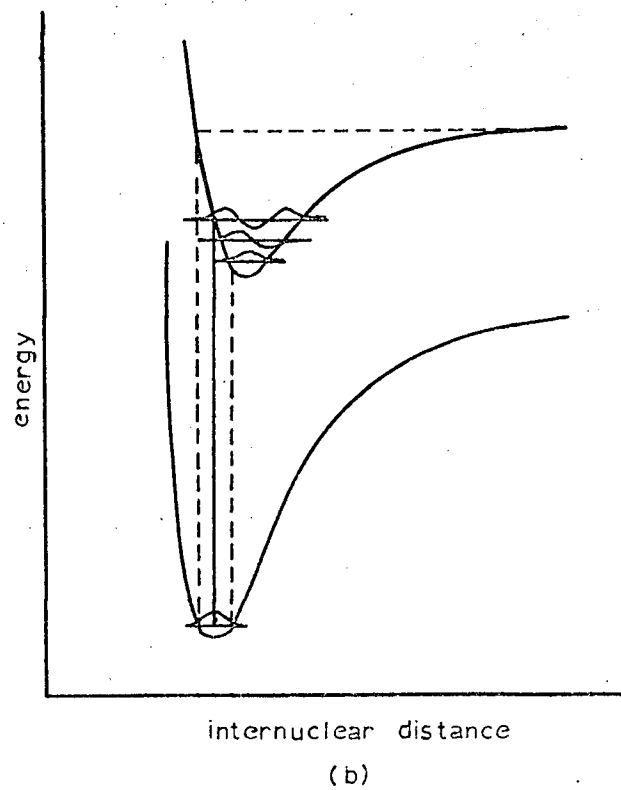
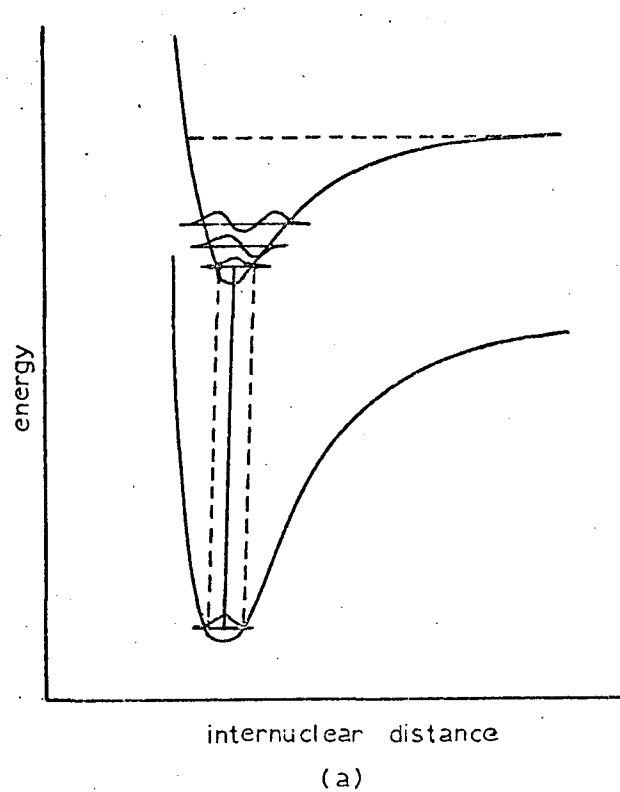


Figure 1. The Franck-Condon Principle

Figure 1(a) represents a transition between two states for which the equilibrium internuclear distances (r_e) are similar. Here, the Franck-Condon principle requires that the probable transition is to the lowest vibrational level of the upper ionic state.

Figure 1(b) shows a moderate change in r_e on formation of the ion. From the diagram it can be seen that the most probable transition would occur to the $v' = 3$ level of the upper electronic state if the Franck-Condon principle holds. However, there will also be transitions to other vibrational levels. Two terms are often used to describe the transitions occurring. A transition to the $v' = 0$ level of the upper electronic state is called an 'adiabatic' transition. This process requires the least amount of energy to reach the appropriate electronic level. The 'vertical' transition corresponds to the most probable transition. It is represented by the solid lines in figure 1. In figure 1(a) the vertical and adiabatic processes are equivalent.

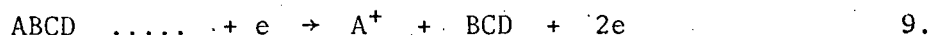
The situation depicted by figure 1(c) shows a large change in r_e . Here the vertical transition intersects the ionic potential energy curve at an energy above the dissociation limit. This results in dissociation of the ion into charged and neutral fragments. This process may be represented as



There is a finite probability of transition over the entire width of the Franck-Condon region. The fragments, therefore, have a spread in kinetic energy.

If a transition occurs to a repulsive ionic curve as shown in figure 1(d) dissociation also occurs.

In the case of polyatomic molecules, potential energy curves are replaced by multidimensional potential energy surfaces. Dissociation occurs first at the weakest bond. Such a process can be written



An electron colliding with an atom or molecule can lose its energy in one of two ways. If an elastic collision takes place, the electron loses part of its energy to the target particle in such a way that the translational energy of the two body system is conserved. Alternatively an inelastic collision may occur in which case a change in the internal energy, within the atom or molecule takes place. An inelastic collision may result in one or more of excitation, ionization and dissociation of the molecule.

The theory of electron-molecule collisions has been described elsewhere (46, 47) and all that will be said is that when the energy of the electron is less than the ionization potential of the system studied, ionization transitions cannot occur and the ionization cross-section is zero. As the energy of the electron is increased above the critical voltage, the cross-section for the transition between the two given levels increases.

C. OPERATION OF THE MASS SPECTROMETER

Many reviews have appeared on the subject of the theory of mass spectrometry (43, 48, 49, 50) and only the "mass spectrometry equations" will be presented here.

The positive ions of mass m (kg) formed in the ion source are accelerated through a potential V (voltage) and the ions acquire kinetic energy eV . If the energy increment is large compared with the initial energy, then

$$eV = \frac{mv^2}{2} \quad 10.$$

where v (m/sec.) is the velocity of the ion after acceleration and e (coulombs) is the charge of the ion.

If the ion now traverses a magnetic field, it will experience a centripetal force, Hev , which is normal to the direction of the magnetic field and to the direction of motion. The result is a circular orbit, such that, the centrifugal force balances the deflecting force

$$\frac{mv^2}{R} = Hev \quad 11.$$

where H (amperes/meter) is the strength of the magnetic field and R (m) is the radius of curvature of the ion beam. Combining equations 10 and 11 v is eliminated and

$$\frac{m}{e} = \frac{R^2 H^2}{2V}$$

or

$$R = \left[\frac{2mV}{eH^2} \right]^{1/2} \quad 12.$$

Thus the ion is deflected with a certain value of R, according to its ratio m/e. Hence, magnetic deflection analyzes according to the momentum of an ion rather than mass alone. Thus for a given mass, variation in V will cause a variation in R and hence a loss in resolution.

The energy band width of the ion beam can be greatly reduced by inserting an electrostatic analyzer in the ion beam before it enters the magnetic field. Thus, if the ion, emerging from the ion source, as described by equation 10 is projected into a radial electrostatic field E (volts/meter) at right angles to the boundary, it will experience a force eE, normal to the direction of motion. The result is a circular orbit of radius r given by:

$$eE = \frac{mv^2}{r}$$

$$\text{or} \quad r = \frac{mv^2}{eE} \quad 13.$$

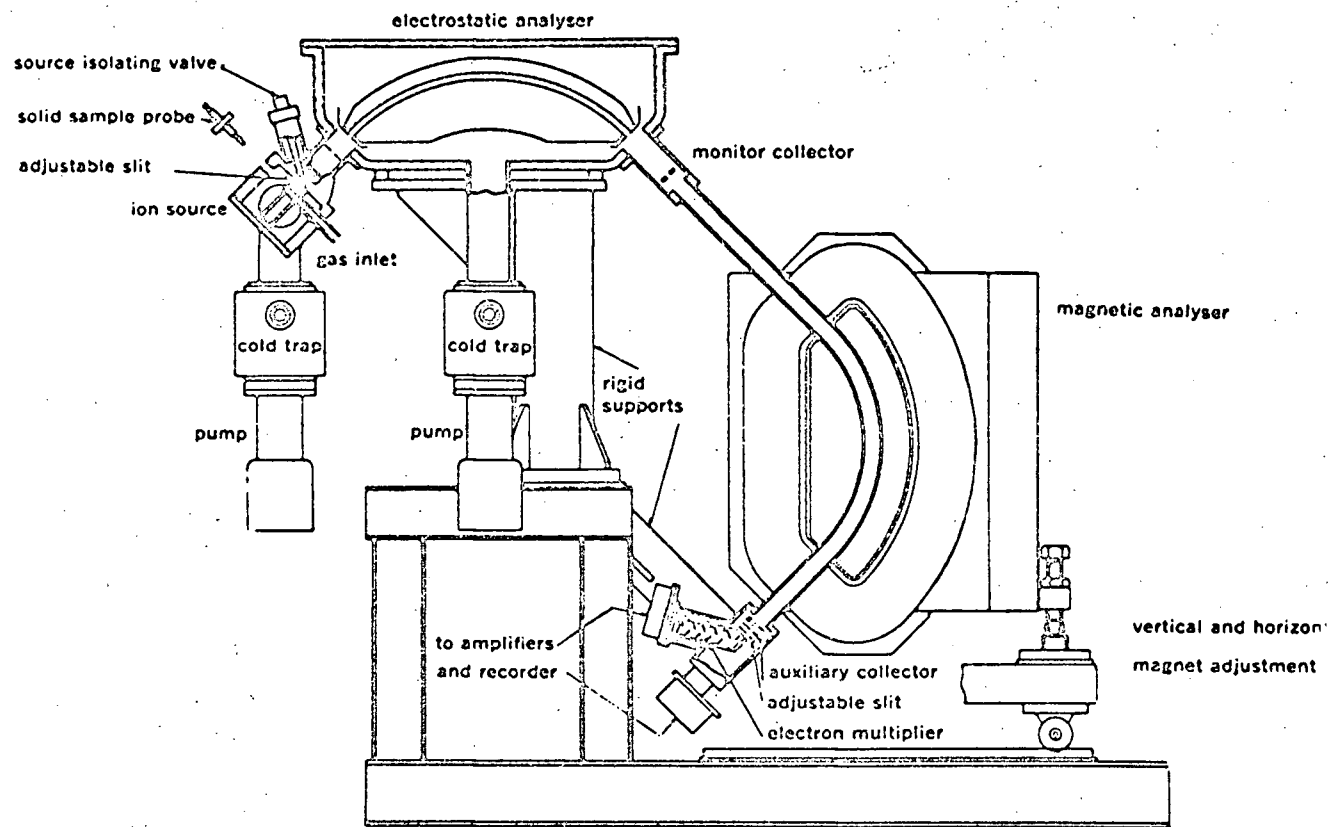
A radial electric field therefore deflects ions according to their kinetic energy and allows ions with a given value of kinetic energy to pass to the magnetic analyzer. Thus instruments, using electrostatic and magnetic fields achieve both velocity and direction focussing and are described as double focussing mass spectrometers.

III EXPERIMENTAL

A. Instrumental

The instrument used for this work is a General Electric-Associated Electrical Industries M.S. 9 mass spectrometer. It is a double focussing, magnetic scanning instrument featuring a resolving power of up to 20,000, controlled by manually variable source and collector slits. Two peaks of equal height are said to be resolved if the valley between them is 10% of their height. Resolving power is then $M/\Delta M$, where M is the average mass and ΔM the mass difference of the peaks. Figure 2 shows the main parts of the instrument which has been fully described elsewhere (51).

The convential electron impact ion source, employing a heated filament, has been replaced with a newly designed dual photoionization - electron impact ion source (52). An exploded view of this ion source is shown in figure 3. In previous photoionization ion sources used in this laboratory (19, 20), it was necessary to replace the electron trap and filament assemblies in the conventional ion source by stainless steel plates containing 3 mm. square apertures. The apertures in the stainless steel plates were necessary for passage of the photon beam which traversed the path normally occupied by the electron beam. To change from electron impact to photoionization operation it was necessary to remove the conventional ion source and replace it with a modified source. In addition, it was also necessary to remove the electron beam collimating magnets since they



Schematic diagram of the Tube Unit of the MS9 Mass Spectrometer

Figure 2. The M.S. 9 Mass Spectrometer.

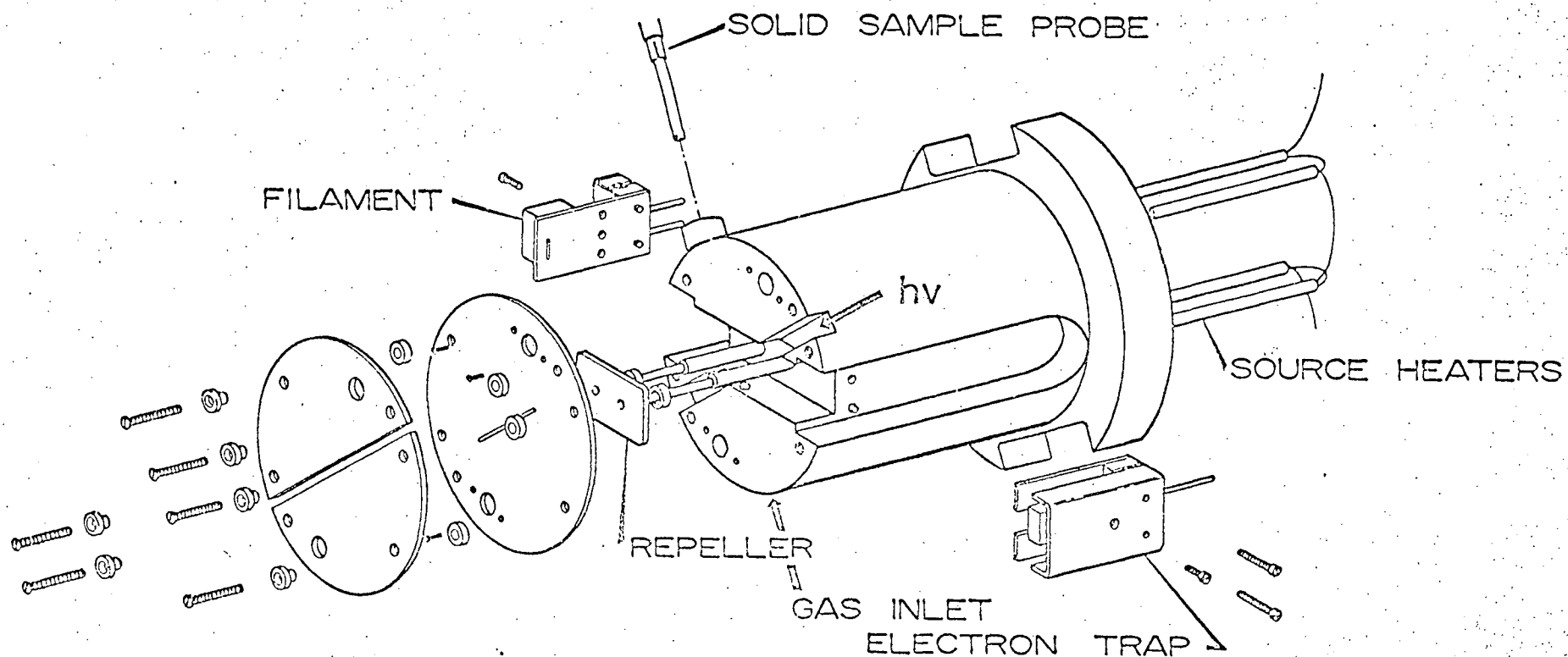


Figure 3.

DUAL PHOTON & ELECTRON IMPACT
ION SOURCE FOR M.S.9.

completely blocked the passage of the photon beam. To make the required changes it was necessary to let the ionization chamber to atmospheric pressure and to remove the source housing. The whole procedure resulted in a heavy loss of machine time. With the dual photon-electron impact ion source, it is no longer necessary to make the above changes. In the new ion source the photon beam traverses the same path as in the standard source except that the mounting of the electron trap and filament assemblies as well as the electron beam collimating magnets have been rotated by 45° . This permits simultaneous use of photoionization and electron impact ionization (53).

One source of photons is a low pressure microwave discharge in helium (He I), it was first used as a far ultraviolet source by Frost and McDowell (54). This provides a line emission spectrum and in the far ultraviolet the majority of the emission has a wavelength of 584.3 \AA , corresponding to an energy of 21.21 e.v. This spectral line arises from the $2^1P \rightarrow 1^1S$ resonance transition in helium (55). The alternative source of photons was a low pressure microwave discharge in a hydrogen-helium mixture. This produces Lyman-alpha radiation (H I), 1215.7 \AA , corresponding to an energy of 10.19 e.v. This spectral line also arises from a $2^1P \rightarrow 1^1S$ transition.

The light source, shown in figure 4, is mounted on the side of a specially modified ion source housing so that the light beam traverses the path formerly occupied by the electron beam in a

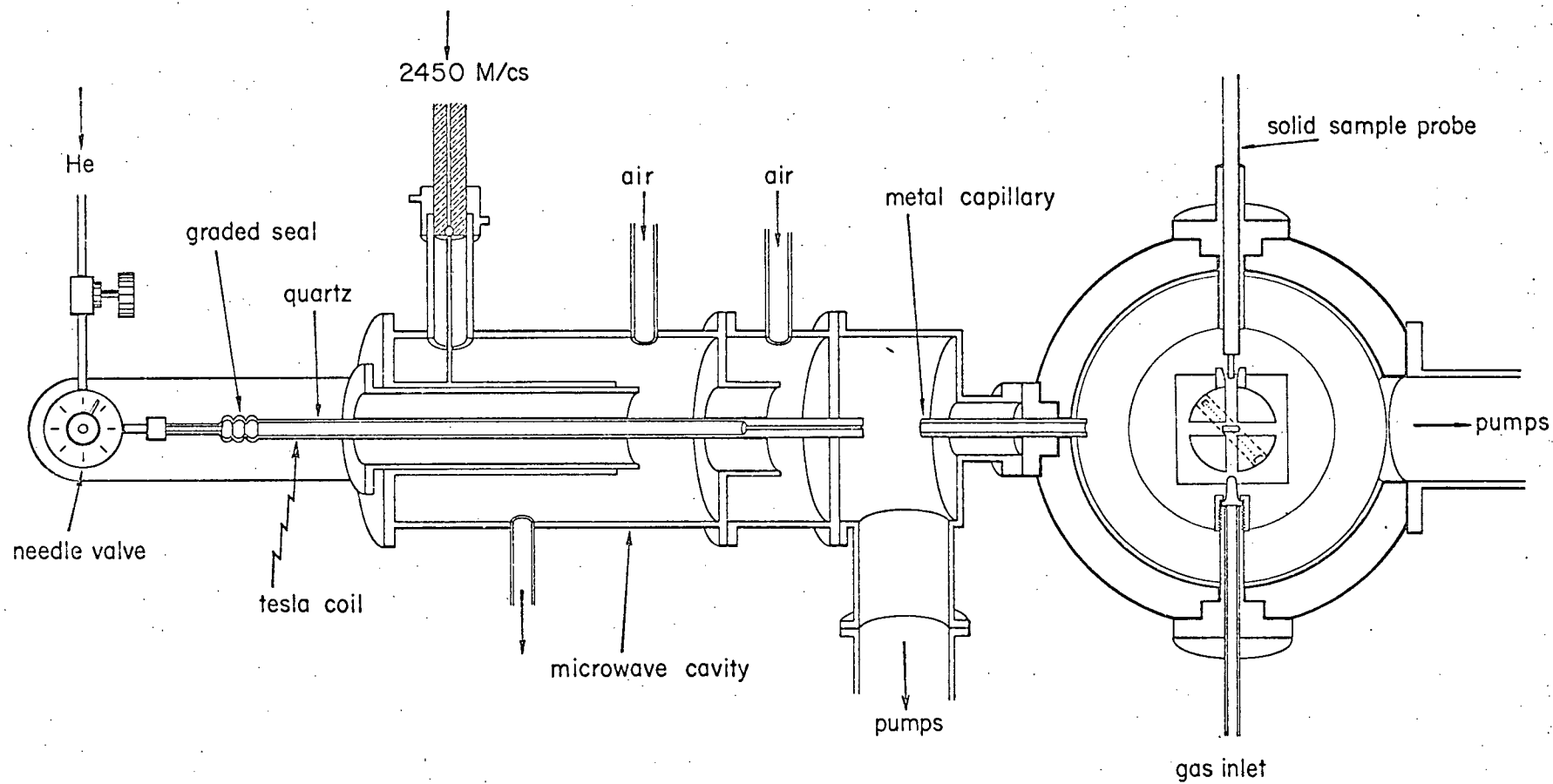


Figure 4.

PHOTOIONIZATION SOURCE (II)

conventional M.S. 9 ion source. A needle valve controls the flow of commercial helium (Canadian Liquid Air Co.) into the quartz tube at a pressure of approximately 1 mm. of Hg. The pressure in the discharge region is also stabilized by a constriction at the other end of the quartz tube. The constriction also serves to facilitate differential pumping of the helium between the light source and the ionization chamber.

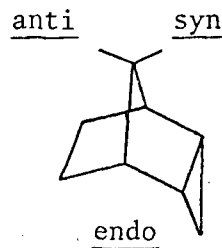
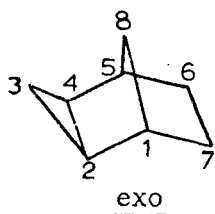
The discharge is produced in the cavity^{by} power from a 'Microtron 200' microwave generator (manufactured by Electro Medical Supplies Ltd., England). This unit produces microwave radiation at a frequency of 2450 Mc./sec. with a maximum power output of 200 watts. The silver plated microwave cavity is constructed of brass and is a modified form of that described by Zelikoff, Wychoff, Auschenbrand and Loomis (56). The discharge is initiated with a Tesla coil. The quartz discharge tube is cooled with compressed air to prevent melting. To prevent excessive helium from entering the mass spectrometer the lower portion of the source consists of a short, earthed brass tube which protrudes through the source housing and has an internal diameter of 2 mm. This capillary transmits a narrow light beam whilst impeding the flow of helium. A 4-cm. pumping line is situated close to the mouth of the capillary and helium is pumped away by a 100 liters/sec. oil diffusion pump backed by a 400 liters/min. mechanical pump. With this arrangement and the optimum helium pressure (that giving the maximum light intensity), the mass spectrometer operating source pressure was about 5.0×10^{-7} mm. Hg. To obtain optimum stability it

was necessary to allow the helium to flow for about 1/4 hour, to purge any residual air.

To produce the Lyman-alpha radiation commercial tank hydrogen (Canadian Liquid Air Co.) was allowed to flow into the light source with the helium light already on. The flow of hydrogen into the system was adjusted using a needle valve until the maximum ion beam was obtained. With this arrangement the mass spectrometric source pressure was about 1.0×10^{-6} mm. Hg. A photon flux of approximately 3.0×10^9 photons/sec. has been reported by Samson (57) in a similar type of source.

B. Samples

This thesis deals with the spectra of some isomeric tricyclo [3.2.1.0^{2,4}] octanes. The numbering of the tricyclo [3.2.1.0^{2,4}] octane ring system is shown below.



The prefixes endo and exo refer to the stereochemistry of the cyclopropane ring relative to the norbornyl ring system, whereas syn and anti refer to the stereochemistry of the substituents at carbon-8 relative to the side of the molecule containing the cyclopropyl ring.

This convention is maintained in compounds containing both a double bond and a cyclopropyl ring. The compounds used in this study are shown in figure 5, they were generously supplied by Drs. J.S. Haywood-Farmer and R.E. Pincock. Abbreviations are used in the figure for some common functional groups. These are: a) acetate, OAc and b) methyl, Me.

The preparation of the compounds shown in figure 5 has been reported (58). Samples to be run on the mass spectrometer were collected, in glass capillary melting point tubes, by gas-liquid partition chromatography using a Wilkins-Aerograph Model A-90-P and a Varian Aerograph 90-P chromatograph, with helium as the carrier gas (flow rate 42 ml./min.) and with thermal conductivity detection. Three columns were used in the chromatographs, at temperatures between 100°C. and 130°C; a 6 ft. x 1/4 in., 1,2,3-tris-(2-cyanoethoxy) propane (20%) on 45/60 mesh chromasorb P (TCEP) column; a 6 ft. x 1/4 in., acid-washed Carbowax 20M (25%) on 60/80 mesh chromasorb W (acid-washed Carbowax) column and a 10 ft. x 3/8 in., Carbowax 20M (20%) on 60/80 mesh chromasorb S (Carbowax prep) column. After collection of the sample, the sample tube was sealed to prevent loss or contamination.

The purity and identification of the compounds had previously been determined by nuclear magnetic resonance using Varian Associates Model A-60 60 Mc. and Model HA-100 100 Mc. spectrometers, by ultraviolet spectroscopy using an Applied Physics Corporation Cary II spectrophotometer, by infrared spectroscopy using a Perkin-Elmer

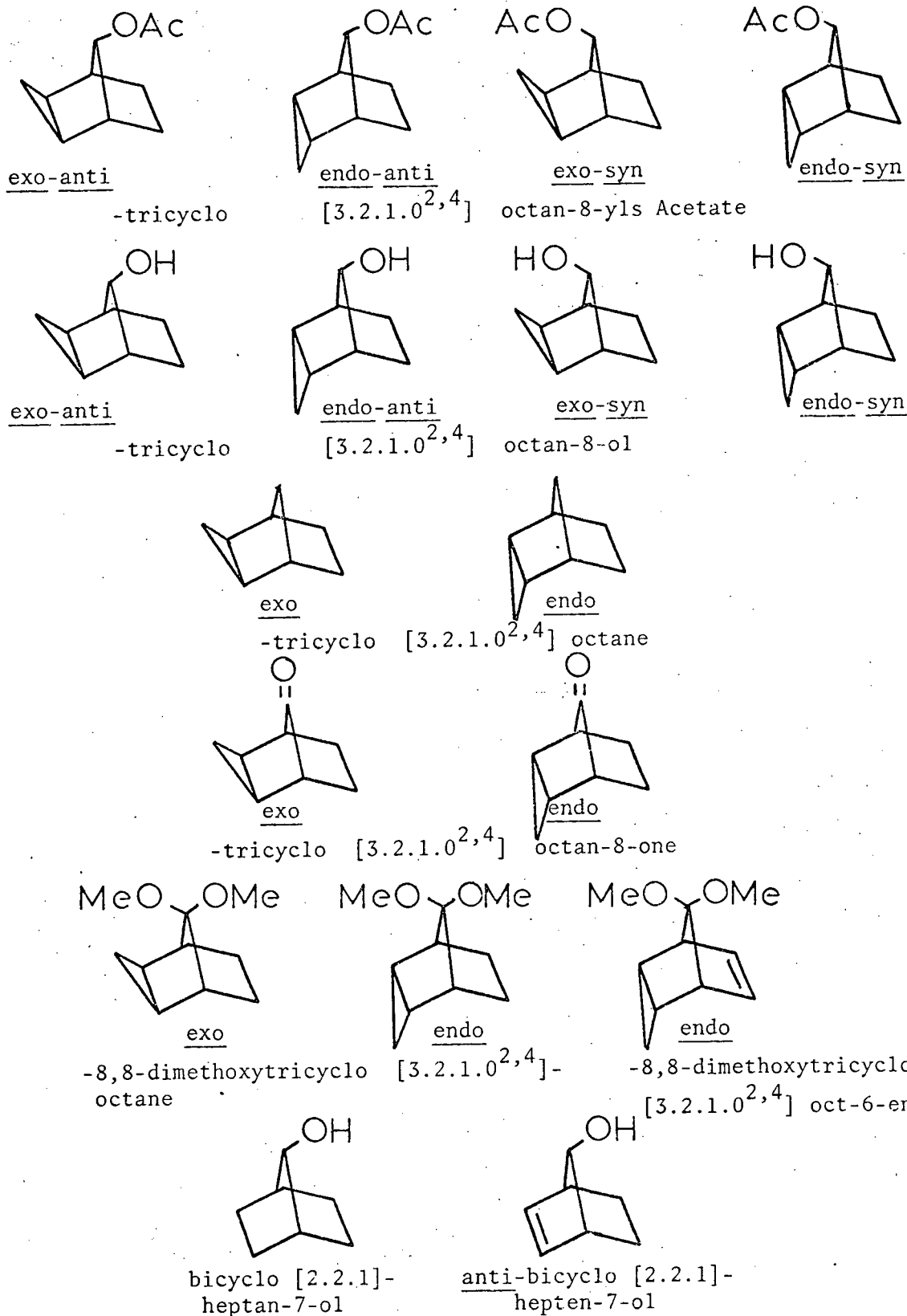


Figure 5. Compounds Studied.

Model 137 B Infracord spectrophotometer with sodium chloride optics and a Perkin-Elmer Model 21 spectrophotometer using matched 0.523 mm. sodium chloride cells. In addition microanalysis and corrected melting points were obtained for all samples. Also no extraneous peaks of mass greater than those associated with the parent were found in the mass spectra of the samples.

C. Mass Spectra

Low resolution mass spectra were obtained for all samples using both the helium resonance line and the hydrogen Lyman-alpha line light sources. All samples were sufficiently volatile at room temperature so that no heating was required and the samples could be introduced into the mass spectrometer through the direct inlet system. The direct inlet system which has no expansion chamber provided a means of introducing small quantities of volatile samples directly into the mass spectrometer ionization chamber. Before any sample was introduced into the instrument, the light source was switched on and the electronics allowed to warm up. With the accelerating voltage at 8 Ke.v. the instrument was focussed on nitrogen at m/e 28, so that the maximum ion beam was obtained at the collector. Also a background spectrum was always recorded before the sample was introduced.

To introduce the sample, one of the sealed melting point capillary tubes, containing 10-20 μl of sample, was opened and the sample-containing tube placed in the direct inlet system. Air and any

non-condensable gases were pumped away by means of freeze-thaw cycles. The amount of sample admitted to the ionization chamber was adjusted using two bellows valves so that the pressure in the source was constant and so that there was sufficient sample to obtain a satisfactory mass spectrum. The total pressure in the source was measured by an ionization gauge, which is located just above the source diffusion pump. When the helium light source was used the total pressure in the source, due to sample and helium, was $2.0-3.0 \times 10^{-6}$ mm. Hg., with the Lyman-alpha light source the total pressure, due to sample and the hydrogen helium mixture, was $2.5 - 3.5 \times 10^{-6}$ mm. Hg. Detailed instructions for the mechanics of running the mass spectrum may be found in the "G.E. - A.E.I. M.S. 9 Mass Spectrometer - Instructions for Operation and Maintenance" manual. The mass spectra of all compounds were recorded under conditions as identical as possible, the band width, recorder paper speed, magnetic scan speed and multiplier settings were the same for all spectra.

The mass spectrometer used in this study employs the peak matching technique for the accurate measurement of the mass of an ion. Knowing the nominal mass of the ion, the relationship between the mass of that ion and that of an accurately known reference is determined by comparison of the ion accelerating voltages necessary to bring the ion beams on to the collector slit, at a constant magnetic field. Provided that the masses of the two ions do not differ by more than 10%, the stability of the circuits and the resolving power of the instrument are sufficient for the measurement of mass ratios with a precision of a few parts in 10^6 .

In this study, in addition to the determination of the exact molecular composition of the parent, the major peaks of the low resolution mass spectra of all samples were 'mass measured' to determine the elemental composition of the ions. The reference compound used was heptacosafuorotributylamine. The high resolution mass measurements were performed using both the helium resonance line and the Lyman-alpha line light sources with a resolution of about 10,000.

D. Ionization Potentials

The method used for the determination of the ionization potentials is similar to that described by Lossing, Tickner and Bryce (59). They found that the semi-log plots of the ionization efficiency curves for the molecule-ions from a number of substances were essentially parallel for voltages in the region of the ionization potential. Since this was the case, they took the ionization potential as the energy at which the ion current was 1% of its value when the electron energy was 50 e.v. Values they obtained were reproducible to ± 0.01 e.v. by this method. Argon was used as the calibrating gas and was introduced simultaneously with the sample under investigation. In this study the ionization potential was taken as the energy at which the ion current is 0.1% of its value when the electron energy is 70 e.v. Argon was also used as the calibrating gas and was introduced into the mass spectrometer along with the sample.

This method while difficult to justify on a theoretical basis provides a convenient method for comparing the ionization

potentials of similar compounds. It is expected that for similar compounds the same quantum states will be available.

IV RESULTS AND DISCUSSION

The explanations given for the differences observed in the relative abundances of the fragments of the isomers are based on the spectra obtained using the helium light source, however, the results obtained when the hydrogen Lyman-alpha resonance line is used as the light source are essentially the same. The differences in intensities of the isomers may be accounted for in most cases in terms of the geometry of the tricyclic systems and the bonding orbitals of the fused cyclopropane ring. The mechanisms used to account for the decomposition of excited ions formed from the molecules are merely empirical rationalizations of gross structural effects applied to the molecules.

A. Ketones

The intensity of the parent ion for the exo isomer is more than twice as great as that of the endo isomer (29% of base peak v. 13% of base peak). This may be seen in figure 6 which shows the spectra obtained for the exo and endo ketones for both light sources. A previous study (60) of the mass spectrum of exo-tricyclo [3.2.1.0^{2,4}] oct-6-en-8-one utilizing a conventional electron impact ion source showed no parent ion. This clearly demonstrates one of the principal advantages of photoionization. If decarbonylation of the molecular ion occurs with equal probability for both isomers it is expected that there will be twice as much of the fragment of m/e 94 (C₇H₁₀⁺)

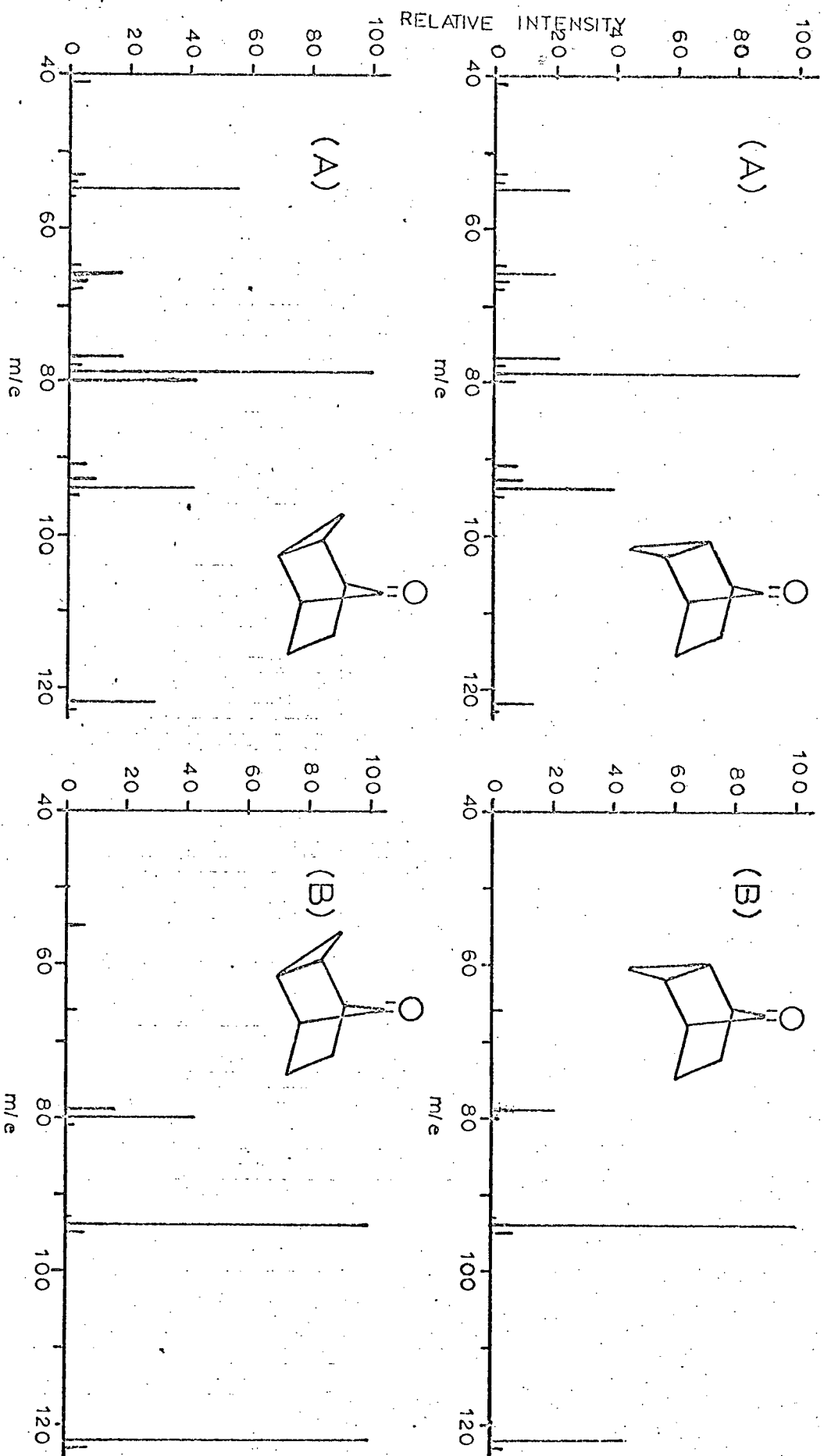


Figure 6. Mass Spectra of Tricyclic Ketones

(a) Helium Light Source (b) Hydrogen Light Source.

present in the exo isomer than in the endo isomer since there is twice as much exo molecular ion. However, there are nearly equal amounts of the decarbonylated fragment. Thus it appears that the endo isomer must undergo decarbonylation more easily than the exo isomer to form a seven membered ring system which is quite stable. Decarbonylation studies of the exo and endo-tricyclo [3.2.1.0^{2,4}]oct-6-en-8-one confirm the greater ease of formation of the seven membered ring system from the endo isomer (60,61,62). The extra stability of the seven membered ring tends to inhibit further fragmentation. The ease of decarbonylation of the isomers and formation of the seven membered ring may be explained in terms of the geometry of the tricyclic systems and the bonding orbitals of the fused cyclopropane ring. In the endo ketone the orbitals forming the cyclopropyl 'banana' bond between carbon-2 and carbon-4 are ideally situated for interaction and subsequent pi bond formation with the p type orbitals available on fragmentation at carbon-1 and carbon-5. Cyclopropyl participation in the decarbonylation step is thus predicted and a concerted process involving simultaneous loss of carbon monoxide and breaking of the cyclopropyl bond can occur to form the seven membered ring system. The geometry of the fused cyclopropyl ring in the exo ketone does not allow overlap of the carbon-2

and carbon-4 bond orbitals with the available p orbitals and cyclopropyl participation is not expected.

Further fragmentation of the exo isomer after decarbonylation is expected since the geometry of the cyclopropane ring in the exo isomer makes it less likely that the formation of the stable seven membered ring will occur. Thus the differences in the relative intensities of the fragments at m/e 80 ($C_6H_8^+$) and at m/e 55 (composed mainly of $C_4H_7^+$) can be rationalized provided that the fragment ions arise from further fragmentation of the decarbonylated fragment.

To account for the equal amounts of base peak at m/e 79, which has the formula $C_6H_7^+$, it is necessary to suppose that one of the bonds of the cyclopropyl ring is broken and a rearrangement occurs to form a methyl group which is then lost. If this occurs the exo and endo isomers will have the same configuration and decarbonylation should then occur with equal probability from either isomer. Thus if the formation and loss of the methyl group occurs with about equal probability in both isomers the amount of fragment at m/e 79 should be nearly equal and this is observed.

B. Methoxy Compounds

It can be seen from figure 7, that within experimental uncertainties, there is no discernible difference in the spectra of the exo and endo isomers of 8,8-dimethoxy [3.2.1.0^{2,4}] octane. The striking feature of the spectra is that there is no peak which is greater than 10% of the base peak. The base peak, at m/e 101, has the formula $C_5H_9O_2^+$ and probably arises by the breaking of the carbon-carbon bonds between carbon atoms 1-8, 6-7 and 4-5.

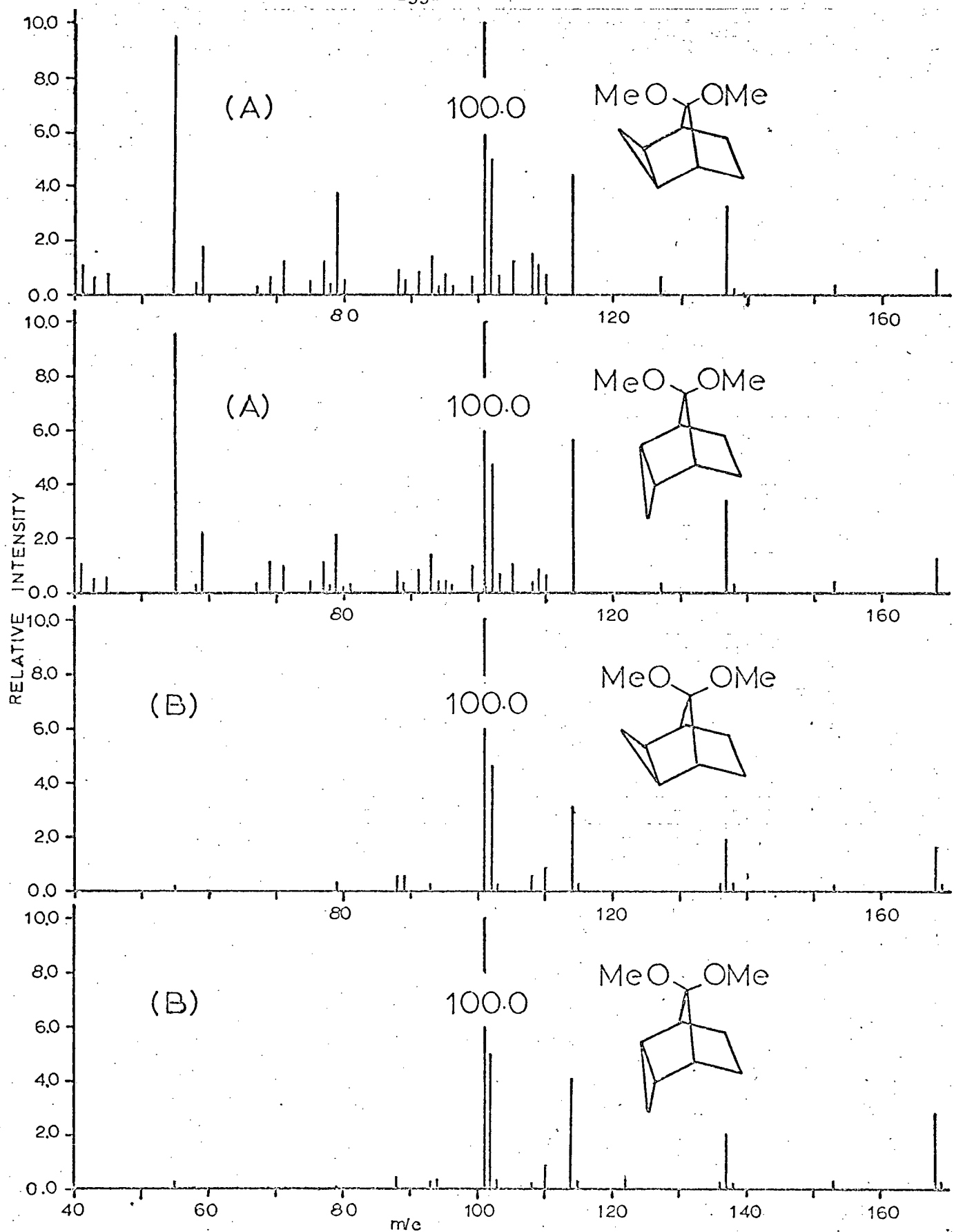


Figure 7. Mass Spectra of Tricyclic Methoxy Compounds.

(a) Helium Light Source (b) Hydrogen Light Source

This appears to be the most probable manner of obtaining the fragment. Additional evidence that the postulated fragmentation scheme is correct may be obtained by the study of the mass spectrum of endo-8, 8-dimethoxy [3.2.1.0^{2,4}] oct-6-ene. It is expected that the fragmentation pattern of this compound, which has a double bond between carbon atoms 6 and 7, would be quite different than that of the saturated isomer if the proposed fragmentation is correct. As may be seen in figure 8 this is the case. The intensity of the fragment at m/e 101 has been considerably reduced and the base peak has been shifted to m/e 91 which has the formula $C_7H_7^+$.

C. Hydrocarbons

From figure 9 it can be seen that there is slightly more parent present for the exo isomer than for the endo isomer (10% of base peak v. 7% of base peak). This may be due to the interaction of the orbitals of the hydrogen atoms of the cyclopropyl ring with those of the hydrogen atoms of carbons 6 and 7 which causes a greater amount of steric interaction in the endo isomer. Due to this steric interactions it would be expected that fragmentation would occur more readily in the endo isomer.

The fragment at m/e 93, which is $C_7H_9^+$, is more intense for the endo isomer than for the exo isomer (31% of base peak v. 23% of base peak). This fragment probably has either a monocyclic seven membered ring structure or a bicyclic norbornene type structure. A seven membered ring is formed more readily for the endo isomer than for the exo isomer because of the overlap of the carbon-2 and carbon-4 bond orbitals with the p type

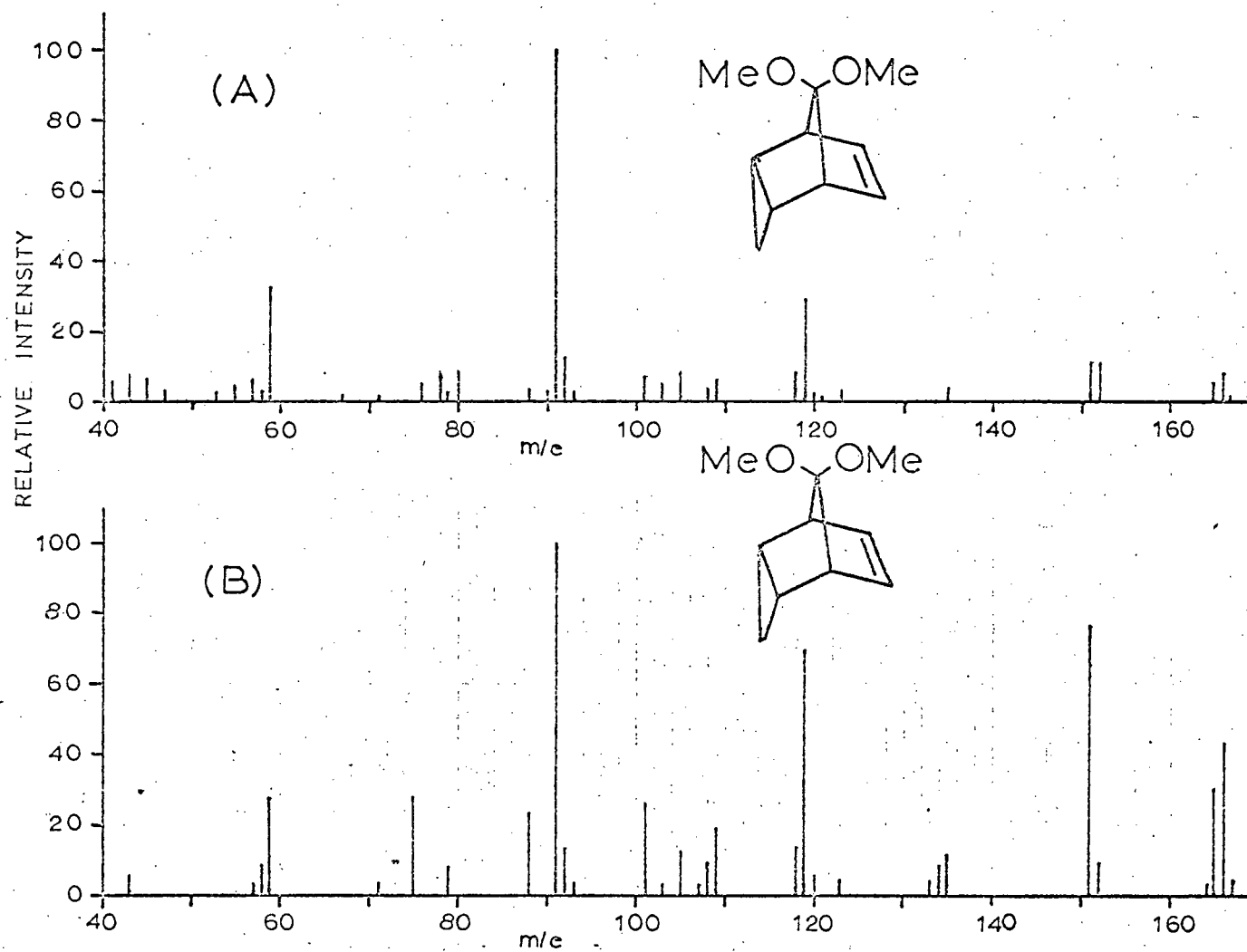
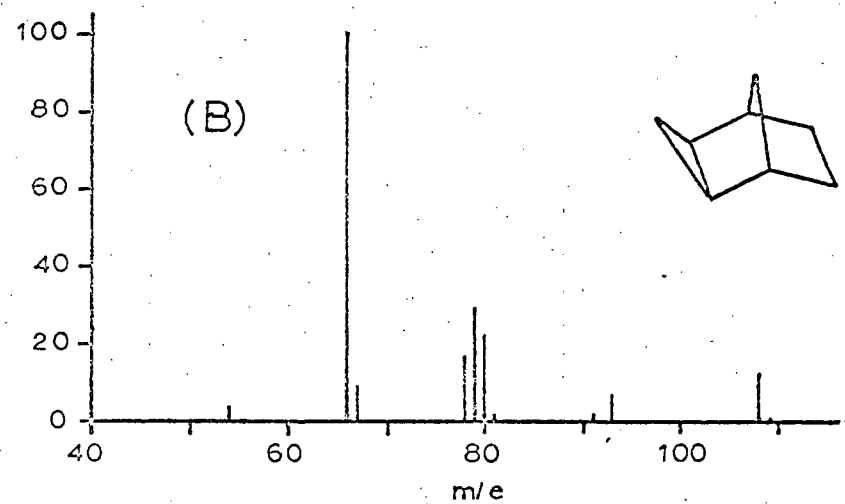
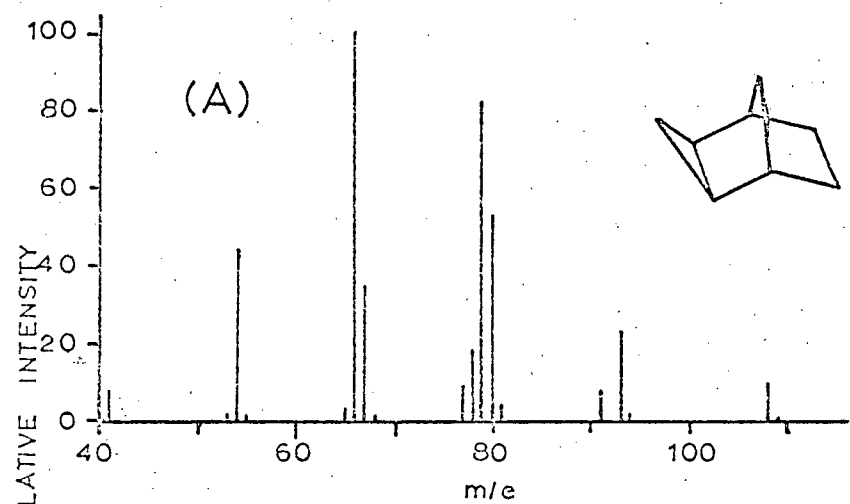


Figure 8. Mass Spectra of Unsaturated Tricyclic Methoxy Compound.
(a) Helium Light Source (b) Hydrogen Light Source



-36-

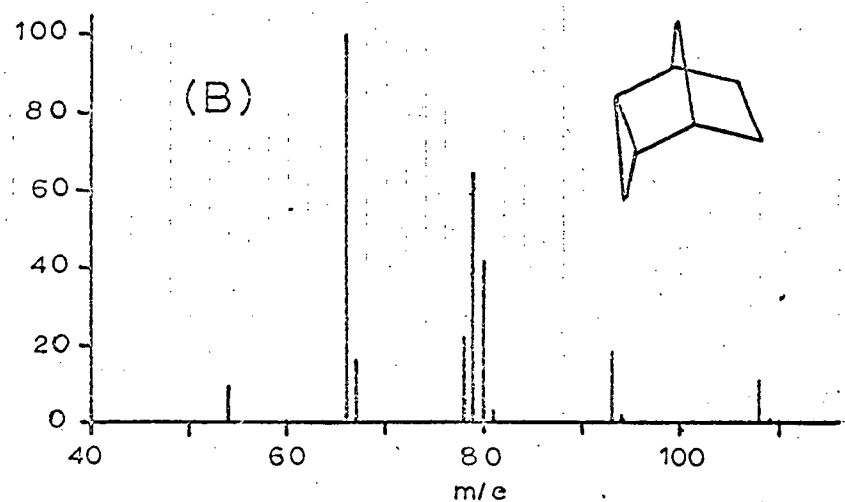
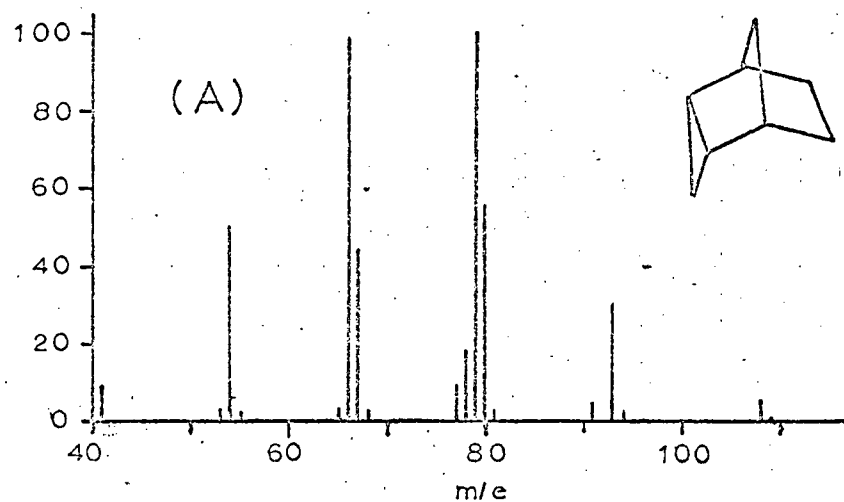


Figure 9. Mass Spectra of Tricyclic Hydrocarbons.

(a) Helium Light Source (b) Hydrogen Light Source

orbitals at carbon-1 and carbon-5 which occurs for the endo isomer and which cannot occur for the exo isomer. The bicyclic system can be formed by loss of a methyl group and if the bicyclic system is formed further fragmentation will occur more readily than for the seven membered ring system. Loss of a CH_2 group would give the fragment at m/e 79 (C_6H_7^+) which is the base peak for the endo isomer and the second largest peak for the exo isomer.

The fragment at m/e 67 is C_5H_7^+ and is more intense for the endo isomer than for the exo isomer (44% of base peak v. 35% of base peak). The greater intensity of the fragment for the endo isomer is probably due to a greater steric interaction in the endo isomer than occurs for the exo isomer.

The base peak for the exo isomer is the fragment at m/e 66 which corresponds to C_5H_6^+ and is only slightly more intense than the endo isomer.

D. Acetates

While it is reasonably easy to compare the spectra of the isomers of the ketones, methoxys and hydrocarbons since only the exo and endo isomers are possible, it is more difficult to compare the spectra of the acetates and alcohols since there are four possible isomers; they are exo-anti, endo-anti, exo-syn and endo-syn. Thus the spectra of the alcohols and acetates may be compared on the basis of the orientation of the cyclopropyl group when the substituent on the 'flagpole' is fixed,

that is, by an exo v. endo comparison, as has been done with the previous compounds or the cyclopropyl group may be held rigid and the orientation of the substituent on the 'flagpole' varied, that is a syn v. anti comparison. In many cases both methods will be employed in an attempt to explain significant differences in the intensities of the fragments present.

The isomeric acetates have the smallest molecular ion intensities of any series of compounds studied. The spectra of the acetates are shown in figures 10 and 11. The low intensity of the molecular ion is probably due to the bulky acetate group which causes more steric interaction than smaller substituents and consequently a less stable molecular ion. The fragment at m/e 124 is predominantly $C_8H_{12}O^+$ and corresponds to the loss of ketene (C_2H_2O) leaving an alcohol type structure. There is more of this fragment present in the spectrum of the endo-anti isomer than in that of the endo-syn isomer (16% of base peak v. 3% of base peak) because in the endo-anti isomer the non-bonding orbitals of the oxygen atom interact with the orbitals of the hydrogen atoms bonded to carbon atoms 6 and 7 to a greater extent than takes place when the interaction occurs with the hydrogen atoms bonded to carbons 2 and 4. This occurs because the hydrogen atoms bonded to carbons 6 and 7, "stick up" out of the plane more than those hydrogen atoms of carbons 2 and 4 do. There is also more of this fragment present in the endo-anti spectrum than is present in the exo-anti spectrum (16% of base peak v. 6% of base peak) probably due to greater steric interaction of the cyclopropyl ring

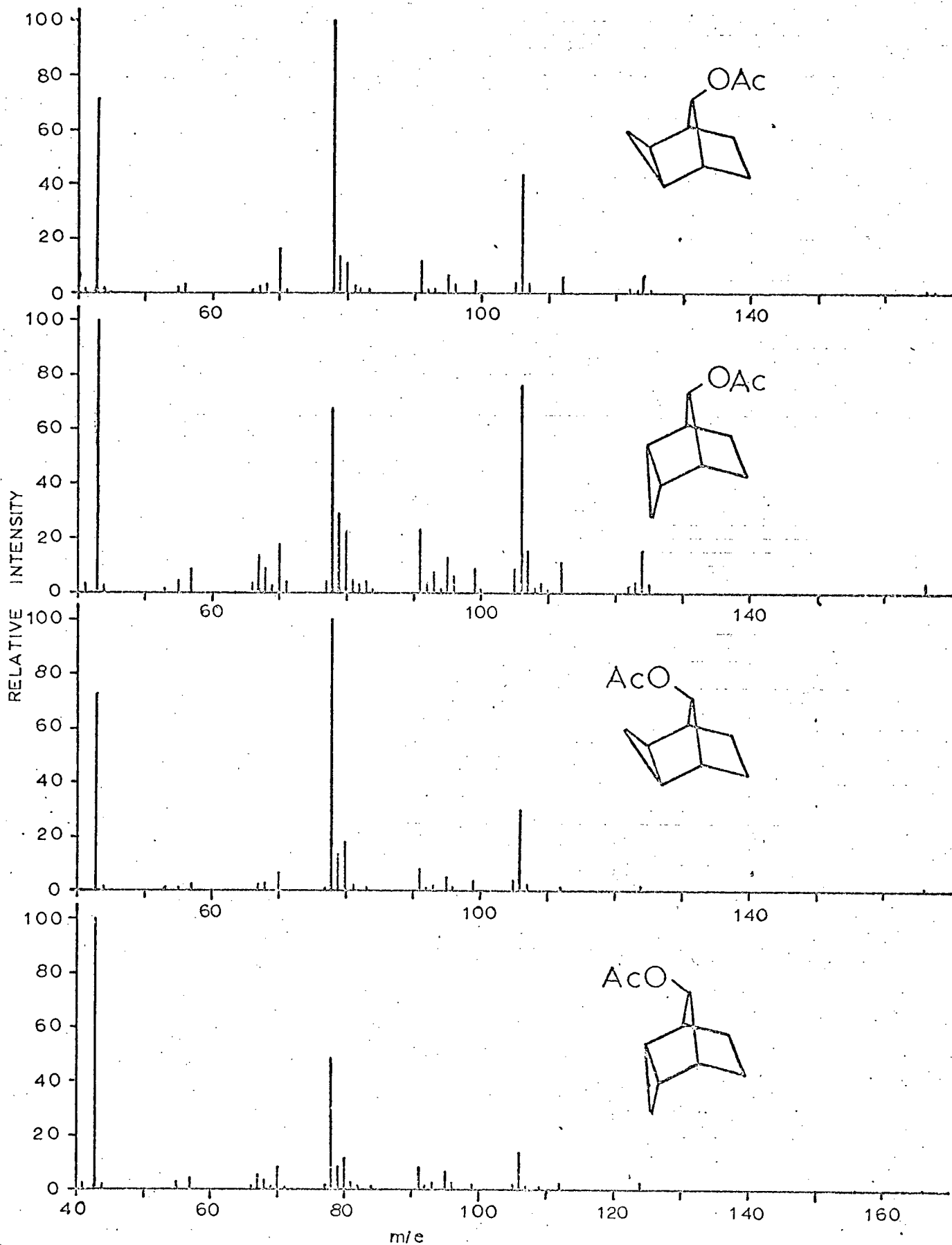


Figure 10. Mass Spectra of Tricyclic Acetates, Helium Light Source.

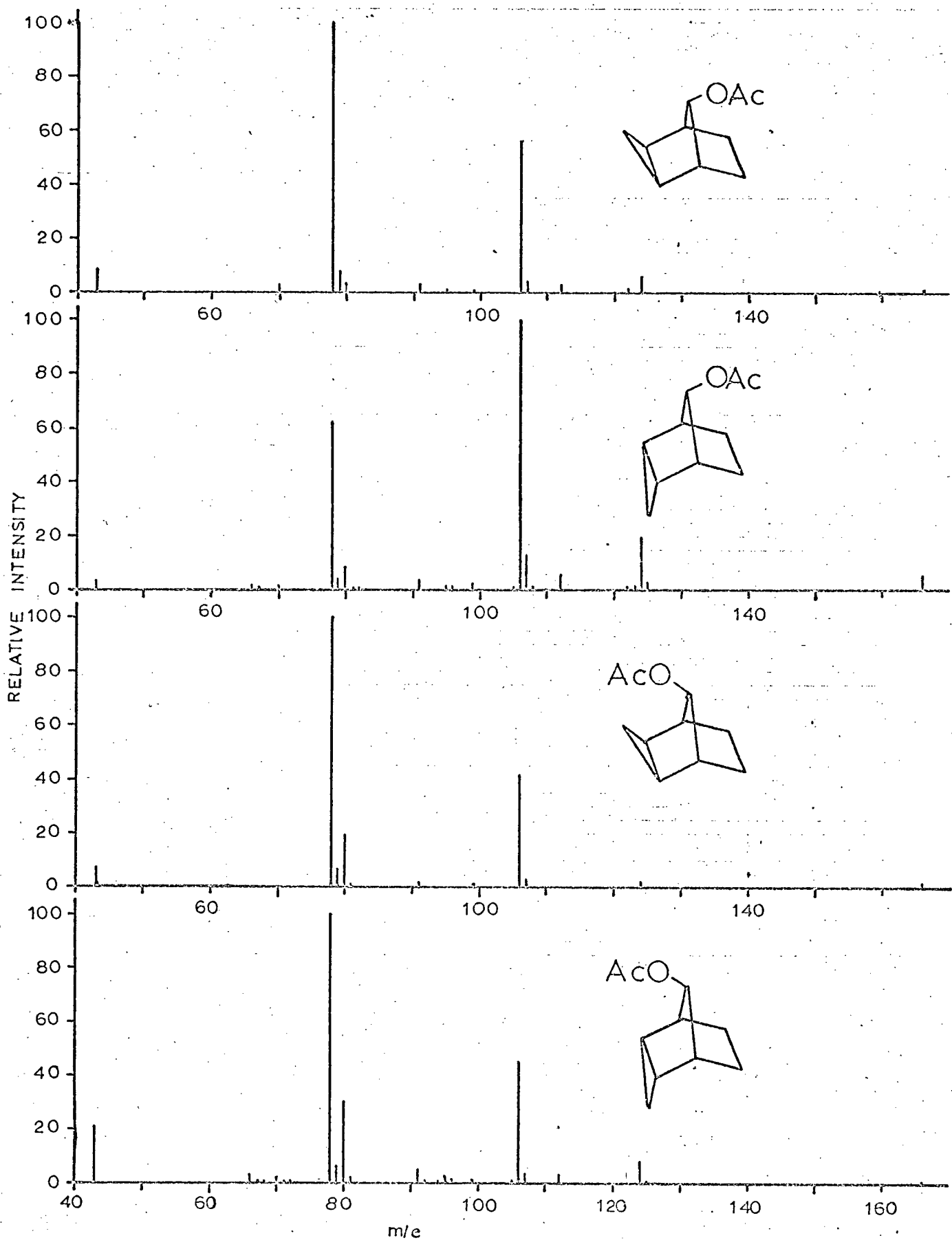


Figure 11. Mass Spectra of Tricyclic Acetates, Hydrogen Light Source.

hydrogen with the hydrogen atoms of carbons 6 and 7 which are below the plane in the endo isomer.

The fragment at m/e 106 has the formula $C_8H_{10}^+$ which corresponds to the loss of acetic acid from the parent, probably by a McLafferty rearrangement (63). As occurs for most fragments the intensity of the endo-anti fragment is the greatest. The amount of fragment for the endo-anti isomer is greater than that for the endo-syn isomer (75% of base peak v. 14% of base peak) probably because there is greater steric interaction of the non-bonding orbitals of the oxygen atom with the orbitals of the hydrogen atoms which are bonded to carbon atoms 6 and 7 in the endo-anti isomer. There is also more of the fragment present for the endo-anti isomer than for the exo-anti isomer (75% of base peak v. 43% of base peak) and this may be due to greater steric interaction of the cyclopropyl group in the endo isomer. There is also more of the fragment at m/e 106 present in the spectrum of the exo-syn isomer than is present in that of the endo-syn isomer (30% of base peak v. 14% of base peak) probably due to the closer proximity of the hydrogen orbitals of the cyclopropyl ring to the non-bonding orbitals of the oxygen atom in the exo-syn isomer. The relative amount of fragment present for the different isomers for the fragments at m/e 80 and 79, which are $C_6H_8^+$ and $C_6H_7^+$ respectively, is very similar to that at m/e 106 and the same reasoning as was used for the fragment at m/e 106 may be employed to explain the differences in the spectra.

The fragment at m/e 91 has the formula $C_7H_7^+$ and probably has a tropylium ion type structure. The intensity of the endo isomers is

greater than that of the corresponding exo isomer because in the endo isomers the orbitals forming the cyclopropyl 'banana' bond between carbons 2 and 4 are ideally situated for interaction and subsequent pi bond formation with the p orbitals at carbons 1 and 5 whereas in the exo isomer they are not.

The trends of the intensities for the various isomers for the fragment at m/e 70, which has the formula $C_4H_6O^+$, are the same as those of the fragment at m/e 124 and similar explanations may be used in an attempt to explain the differing intensities for the various isomers.

The base peak for the exo isomers is at m/e 78 and corresponds to the fragment $C_6H_6^+$ while the base peak for the endo isomers is at m/e 43 and has the formula $C_2H_3O^+$. The difference in base peak may be accounted for on the basis of the formation of a seven membered ring for the endo isomer which occurs to a lesser extent in the exo isomer.

If the bond between carbon atoms 1 and 8 or 5 and 8 is broken, there is a greater probability of forming a seven membered ring in the endo isomers because the cyclopropyl 'banana' bond between carbon atoms 2 and 4 is ideally situated for interaction and subsequent pi bond formation with the developing p orbital at carbon 1 or 5 whereas in the exo isomer the geometry of the fused cyclopropyl ring does not allow overlap of the bond orbitals of carbons 2 and 4 with the developing p orbitals. Once the formation of the 7 membered ring has occurred it is unlikely that the fragment at m/e 78 will be formed. Thus it is expected that the intensity of the fragment will be greater for the exo isomer.

The fragment at m/e 43 which is the base peak for the endo isomers is the second most intense peak in the spectra of the exo isomers. It arises by the breaking of the carbon-oxygen bond and retention of the positive charge by the oxygen atom of the acetate group.

E. Alcohols

Only small differences are observed in the intensity of the molecular ion in the spectra of the isomeric alcohols as may be seen from figures 12 and 13 and because the absolute intensity is quite small no attempt is made to explain these differences. The fragment at m/e 106 has the formula $C_8H_{10}^+$ and corresponds to the loss of water from the molecular ion. Biemann (1) has suggested that in the process of water elimination from alcohols which occurs in the mass spectrometer occurs such that for epimeric polycyclic alcohols, such as borneol and isoborneol, the one with the most sterically hindered hydroxyl function exhibits the lower intensity molecular ion and the higher intensity $M-H_2O$ (parent ion minus water) peak. This effect is not observed with the tricyclic alcohols used in this study probably due to the geometry of the tricyclic system which leads to other steric interactions. The intensity of the molecular ion minus water peak in the endo-syn spectrum is greater than that in the exo-syn spectrum (40% of base peak v. 24% of base peak) and the intensity in the endo-anti spectrum is greater than that in the exo-anti spectrum (31% of base peak v. 20% of base peak). Also there is slightly more of this fragment present in the spectrum of the exo-syn isomer than in that of the exo-anti (24% of base peak v. 20% of base peak), similarly the endo-syn isomer has a more intense peak

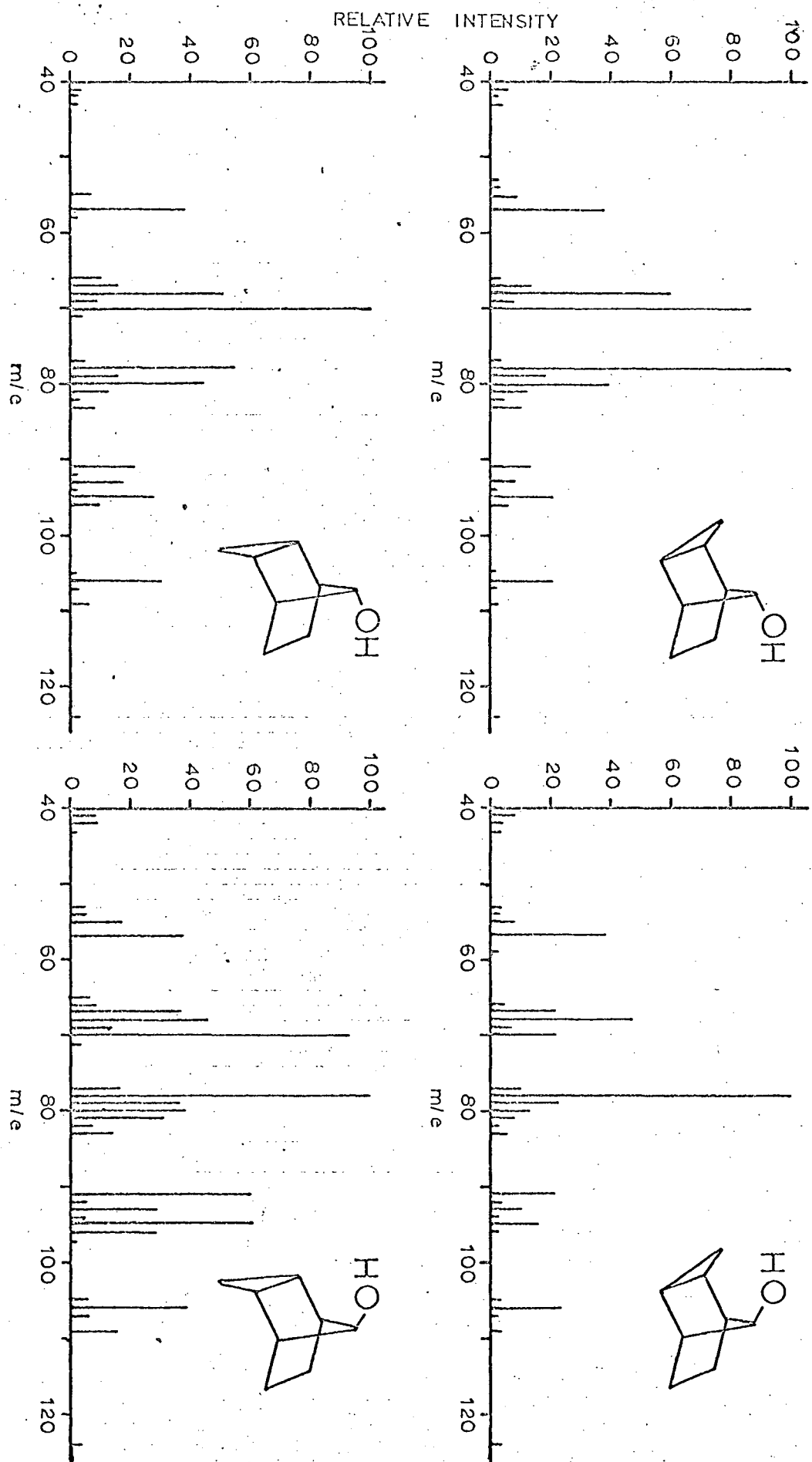


Figure 12. Mass Spectra of Tricyclic Alcohols, Helium Light Source.

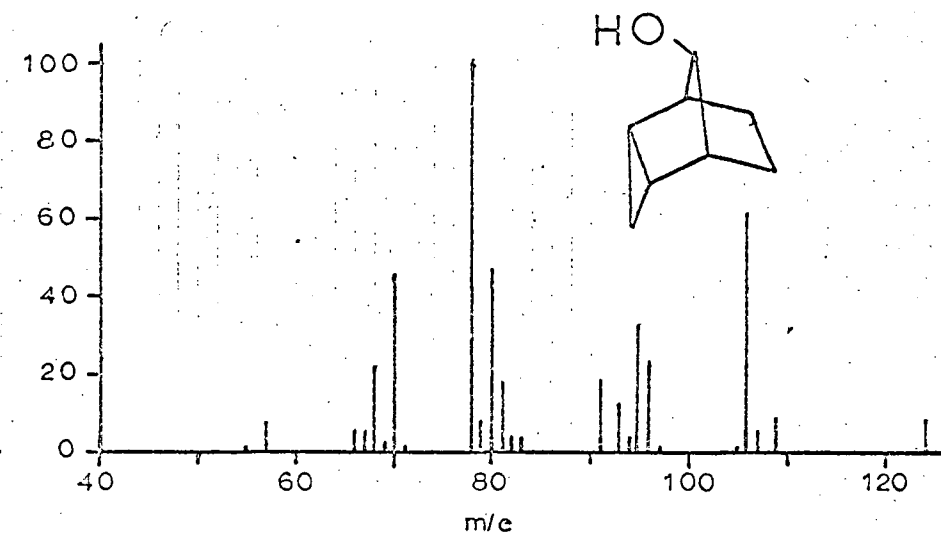
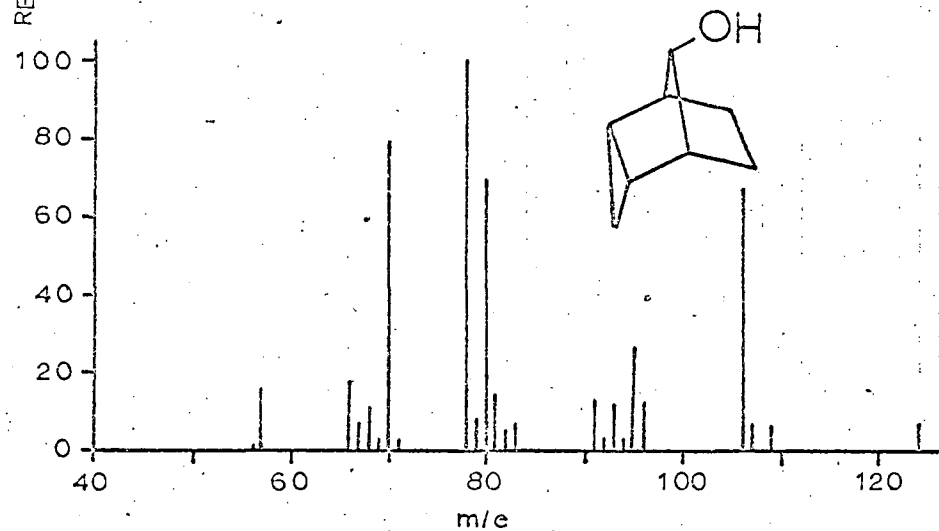
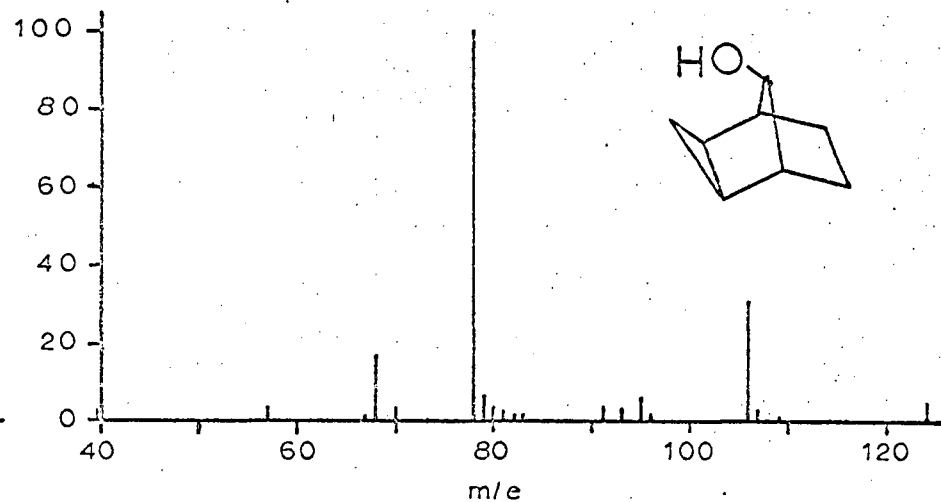
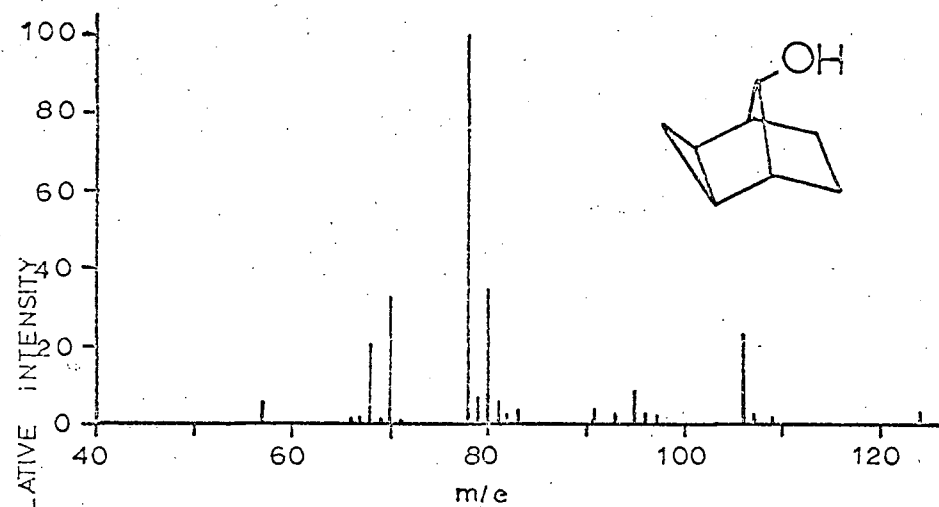


Figure 13. Mass Spectra of Tricyclic Alcohols, Hydrogen Light Source.

than the endo-anti isomer. There appears to be a direct correlation between the intensity of the molecular ion minus water fragment and the ease of formation of a seven membered ring. The endo isomers form the seven membered ring more easily than the exo isomers because in the endo isomers the orbital forming the cyclopropyl 'banana' bond are ideally situated for interaction and subsequent pi bond formation whereas this is not the case with the exo isomers. Also the intensity of the molecular ion minus water fragment is greater in the spectrum of the syn isomer than in the corresponding anti isomer due to the fact that the hydrogen lost in the formation of water is from the syn side of the molecule, the formation of a seven membered ring is facilitated.

The fragment which occurs at m/e 95 is a doublet consisting of $C_7H_{11}^+$ and $C_6H_7O^+$. The $C_7H_{11}^+$ fragment corresponds to the loss of COH from the molecular ion and may only arise by a rearrangement process. Because the intensity of the fragment is greater in the endo-anti spectrum than in that of the exo-anti (13% of base peak v. 9% of base peak) and the intensity of the endo-syn is greater than that of exo-syn (37% of base peak v. 8% of base peak) it is expected that a seven membered ring is involved in the fragmentation process. The $C_6H_7O^+$ fragment arises by the loss of C_2H_5 from the molecular ion. If the loss occurs in two stages, first the loss of C_2H_4 and then the loss of a hydrogen radical, then the C_2H_4 lost is probably that of carbons 6 and 7. The p orbitals of the cyclopropyl group of the endo isomers are in a position which facilitates the formation of a double bond in a six membered ring more easily than occurs in the case of the exo isomers. Thus it is expected

that the endo isomers will have more intense peaks than the corresponding exo isomer. The six membered ring arising from the endo isomers will probably be in a chair type configuration while that arising from the exo isomer will be in a boat type configuration. If the fragment at m/e 77 arises predominantly from the loss of water from the fragment at m/e 95 ($C_6H_7O^+$) then, using similar reasoning to that used by Brion and Hall (18), who account for the loss of water from the isomers of t-butylcyclohexanol on the basis of configuration, it would be expected that the syn isomer would have more intense m/e 77 peaks than the corresponding anti isomer and this is observed. Also it is to be expected that the exo-syn isomer if it has boat symmetry will exhibit a more intense m/e 77 peak than the endo-syn if the latter has chair symmetry. However, the intensity of the endo-syn isomer is greater than that of the exo-syn isomer (17% of base peak v. 11% of base peak). This behaviour may be accounted for on the basis that the fragment at m/e 95 is the precursor of the fragment at m/e 77. For the fragment at m/e 95 the endo-syn isomer is more than three times as intense as the exo-syn isomer (25% of base peak v. 8% of base peak), thus if the intensity of the fragment at m/e 95 was the same for both isomers it would be expected that the exo-syn isomer would be more intense than the endo-syn isomer.

The fragment at m/e 91 has the formula $C_7H_7^+$ and probably has a tropylium ion type structure. As with previous fragments the intensity of the endo-syn isomer is greater than that of the exo-syn isomer (61% of base peak v. 22% of base peak) and the intensity of the endo-anti

is greater than that of the exo-anti isomer (22% of base v. 14% of base peak). The more intense peaks occur for the endo isomers because the orbitals forming the cyclopropyl 'banana' bond are ideally situated for interaction and subsequent pi bond formation whereas in the exo isomer they are not. In addition, the intensity of the fragment is greater for the exo-syn isomer than for the exo-anti isomer (22% of base peak v. 14% of base peak) and similarly the intensity of the endo-syn isomer is greater than that of the endo-anti isomer (61% of base peak v. 22% of base peak). The intensity of the peak in the syn isomer is greater than in the corresponding anti isomer because elimination of the hydroxyl group occurring from the syn side of the molecule facilitates the formation of a seven membered ring system.

The fragment at m/e 80 is $C_6H_8^+$ and follows the same trend as the other fragments in that the intensity of the endo isomer is greater than that of the corresponding exo isomer. However, for this fragment the abundance of the anti isomer is greater than that of the corresponding syn isomer which may arise because the elimination of the hydroxyl group occurs by a different mechanism than occurs for the other fragments.

The base peak for the exo-anti, exo-syn and endo-syn isomers and the second largest peak in the spectrum of the endo-anti isomer is the fragment which occurs at m/e 78 and which is $C_6H_6^+$. The base peak for the endo-anti isomer occurs at m/e 70 and has the formula $C_4H_6O^+$. The amount of this fragment present for the endo-anti isomer is greater than that for the exo-anti isomer and the amount present in the endo-syn spectrum is greater than that in the exo-syn spectrum. The greater intensity

of the fragment for the endo isomers than for the corresponding exo isomer indicates the probable formation of a seven membered ring as an intermediate.

The fragment at m/e 68 corresponds to $C_5H_8^+$ and can only arise if a rearrangement process occurs. Since deuterated compounds were not used in this study the rearrangement that occurs cannot be identified.

The peak at m/e 57 is $C_3H_5O^+$ for which the intensity in all isomers is the same within experimental error.

The spectra of bicyclo [2.2.1] heptan-7-ol and anti-bicyclo [2.2.1] hepten-7-ol are shown in figure 14 and are included for comparison with the tricyclic alcohols. The spectrum of bicyclo [2.2.1] heptan-7-ol is very similar to that of the isomeric tricyclic alcohols in that many of the same fragments are present in both cases although their intensities are different. The fragments in common are: the molecular ion minus water, those at m/e 70 ($C_4H_6O^+$), m/e 68 ($C_5H_8^+$) and m/e 57 ($C_3H_5O^+$). It is not surprising that the other major fragments of the tricyclic alcohols are not present in the spectrum of the bicyclic compound since seven membered rings were postulated to account for these fragments and the seven membered ring cannot be easily formed from the bicyclic compound. The base peak for the bicyclo [2.2.1] heptan-7-ol is the molecular ion minus water fragment at m/e 94. The other major peaks in the spectrum are at m/e 79 and m/e 81 which are $C_6H_7^+$ and $C_6H_9^+$ respectively.

The spectrum of anti-bicyclo [2.2.1] hepten-7-ol also has fragments at m/e 79 and m/e 81. The peak at m/e 79 is $C_6H_7^+$ and is the base peak for the spectrum. The peak at m/e 81 is a doublet consisting of

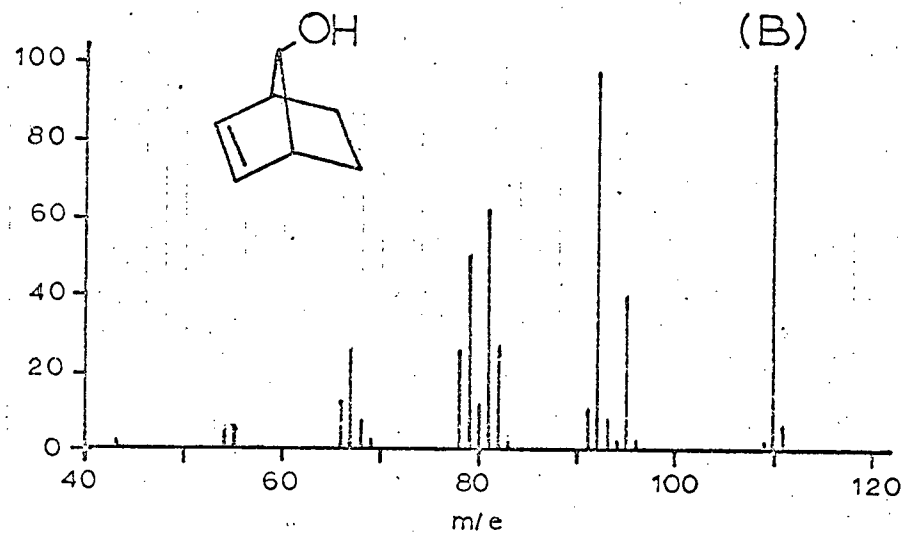
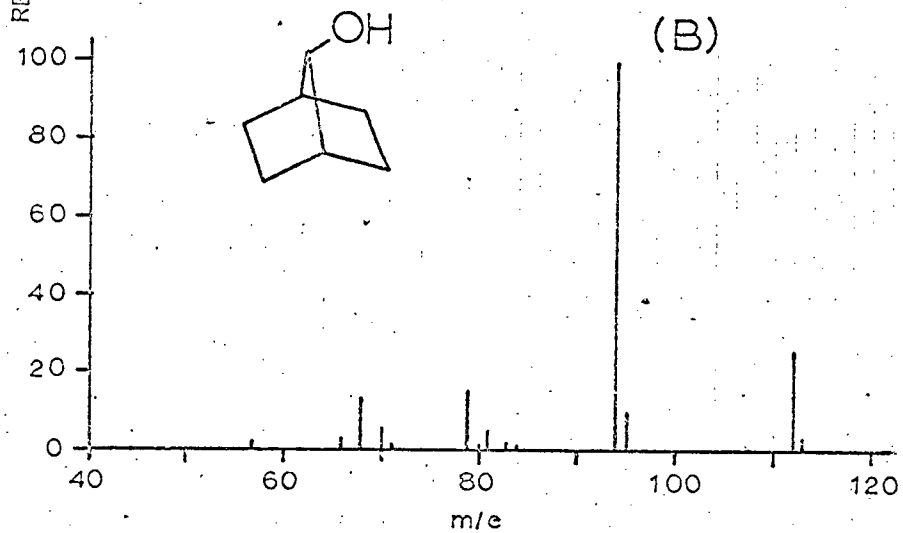
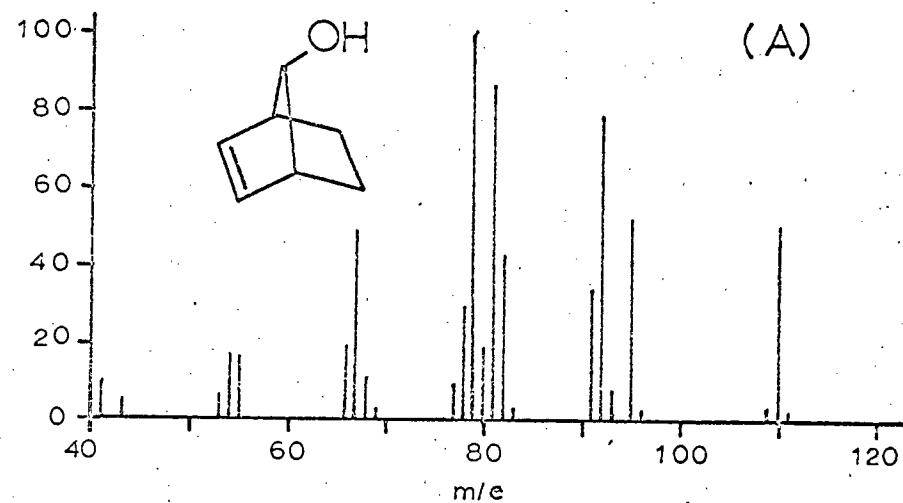
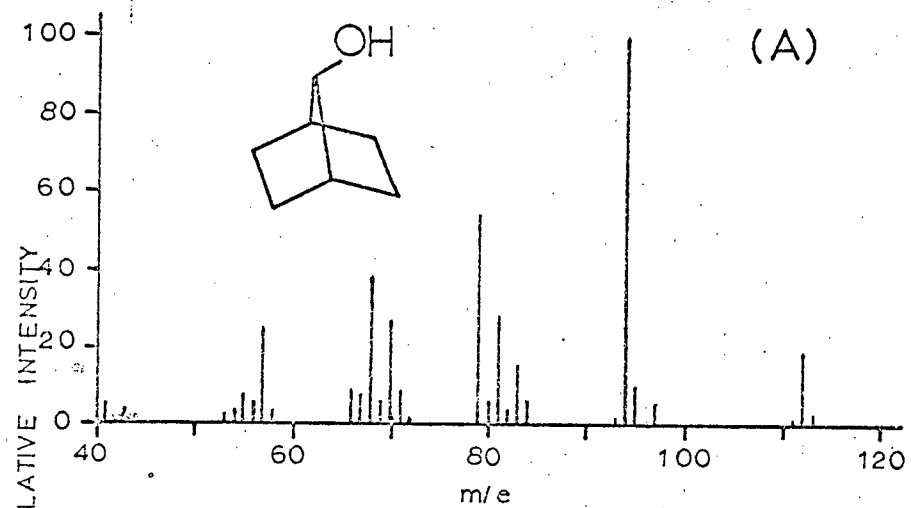


Figure 14. Mass Spectra of Bicyclic Alcohols.

(a) Helium Light Source

(b) Hydrogen Light Source

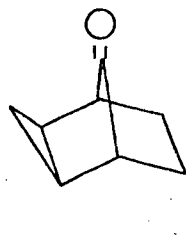
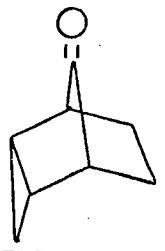
$C_5H_5O^+$ and $C_6H_9^+$ which are present in the ratio 1:5 when the helium light source is used. In common with the isomeric tricyclic alcohols there is an abundant molecular ion minus water peak which occurs at m/e 92 in the spectrum. Also in common with the tricyclic alcohols is the fragment at m/e 95 which has the formula $C_6H_7O^+$. The other major peaks in the spectrum are those at m/e 82 ($C_5H_6O^+$ and $C_6H_{10}^+$ present in the ratio 4:1 respectively, for the helium light source) and at m/e 67 ($C_5H_7^+$). There is no apparent correlation of these fragments with either the tricyclic alcohols or with bicyclo [2.2.1] heptan-7-ol.

F. High Resolution

The high resolution mass spectrometer results for the compounds used in this study are shown in tables 1-6. In addition to the determination of the molecular composition of the molecular ion, the composition of the major fragments in the low resolution mass spectra were also determined.

The lines in the table indicate that no attempt was made to determine the composition of the fragment ion because of insufficient intensity. The doublets observed are shown in the tables together with their relative ratios. For example, in the spectrum of endo-syn tricyclo [3.2.1.0^{2,4}] octan-8-ol a doublet occurs at m/e 95 which is composed of $C_7H_{11}^+$ and $C_6H_7O^+$. For the helium light source the $C_7H_{11}^+$ and $C_6H_7O^+$ fragments are present in the ratio 3:2 whereas for the hydrogen light source the ions are present in the ratio 1:1.

In a number of instances a knowledge of the elemental composition of a fragment permits the formulation of a probable fragmentation scheme



m/e

122

$C_8H_{10}O$

$C_8H_{10}O$

94

C_7H_{10}

C_7H_{10}

80

C_6H_8

C_6H_8

79

C_6H_7

C_6H_7

77

C_6H_5

C_6H_5

66

C_5H_6

C_5H_6

55

C_4H_7

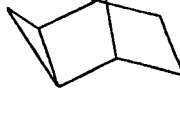
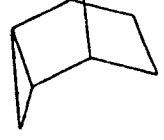
C_4H_7

C_3H_3O (Trace)

C_3H_3O (Trace)

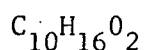
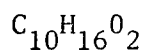
TABLE I

High Resolution Results for Tricyclic Ketones

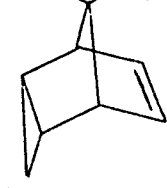
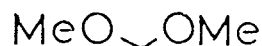
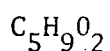
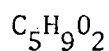


m/e

168

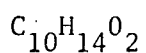


101



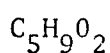
m/e

166

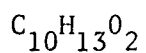


m/e

101



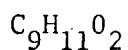
165



92



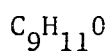
151



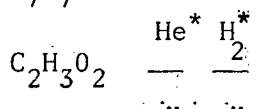
91



135



59



119



2 1

TABLE II

High Resolution Results for Saturated and Unsaturated Tricyclic Methoxy Compounds

* See Text for explanation

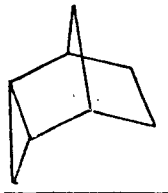
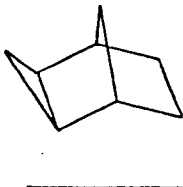
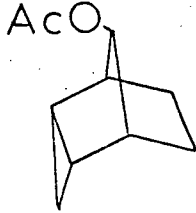
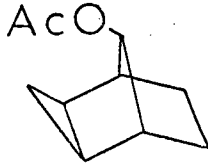
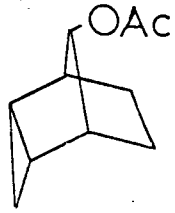
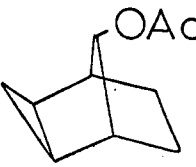
<u>m/e</u>		
108	C_8H_{12}	C_8H_{12}
93	C_7H_9	C_7H_9
91	C_7H_7	C_7H_7
80	C_6H_8	C_6H_8
79	C_6H_7	C_6H_7
78	C_6H_6	C_6H_6
67	C_5H_7	C_5H_7
66	C_5H_6	C_5H_6
54	C_4H_6	C_4H_6

TABLE III

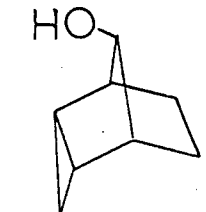
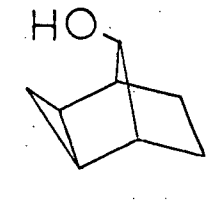
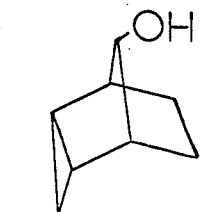
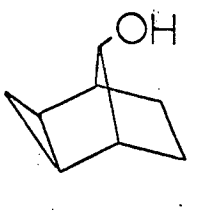
High Resolution Results for Tricyclic Hydrocarbons

m/e				
166	$C_{10}H_{14}O_2$	$C_{10}H_{14}O_2$	$C_{10}H_{14}O_2$	$C_{10}H_{14}O_2$
124	$C_8H_{12}O$ $C_7H_8O_2$ (Trace)	$C_8H_{12}O$ $C_7H_8O_2$ (Trace)	$C_8H_{12}O$ $C_7H_8O_2$ (Trace)	$C_8H_{12}O$ $C_7H_8O_2$ (Trace)
106	C_8H_{10}	C_8H_{10}	C_8H_{10}	C_8H_{10}
91	C_7H_7	C_7H_7	C_7H_7	—
80	C_6H_8	C_6H_8	C_6H_8	C_6H_8
79	C_6H_7	C_6H_7	C_6H_7	C_6H_7
78	C_6H_6	C_6H_6	C_6H_6	C_6H_6
	$\underline{\text{He}^*} \quad \underline{\text{H}_2^*}$	$\underline{\text{He}^*} \quad \underline{\text{H}_2^*}$	$\underline{\text{He}^*} \quad \underline{\text{H}_2^*}$	$\underline{\text{He}^*} \quad \underline{\text{H}_2^*}$
70	C_4H_6O 1 only $C_3H_2O_2$ Trace	C_4H_6O 1 only $C_3H_2O_2$ Trace	C_4H_6O 1 only $C_3H_2O_2$ Trace	C_4H_6O 1 only $C_3H_2O_2$ Trace
43	C_2H_3O	C_2H_3O	C_2H_3O	C_2H_3O

* See text for explanation.

TABLE IV

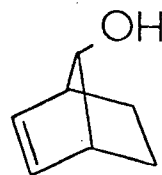
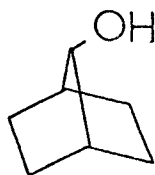
High Resolution Results for Tricyclic Acetates

																												
m/e																												
124	$C_8H_{12}O$	$C_8H_{12}O$	$C_8H_{12}O$	$C_8H_{12}O$																								
106	C_8H_{10}	C_8H_{10}	C_8H_{10}	C_8H_{10}																								
95	<table><tr><td>C_7H_{11}</td><td>$\frac{He^*}{3}$</td><td>$\frac{H_2^*}{2}$</td></tr><tr><td>C_6H_7O</td><td>$\ddot{2}$</td><td>$\ddot{1}$</td></tr></table>	C_7H_{11}	$\frac{He^*}{3}$	$\frac{H_2^*}{2}$	C_6H_7O	$\ddot{2}$	$\ddot{1}$	<table><tr><td>C_7H_{11}</td><td>$\frac{He^*}{1}$</td><td>$\frac{H_2^*}{1}$</td></tr><tr><td>C_6H_7O</td><td>$\ddot{1}$</td><td>$\ddot{1}$</td></tr></table>	C_7H_{11}	$\frac{He^*}{1}$	$\frac{H_2^*}{1}$	C_6H_7O	$\ddot{1}$	$\ddot{1}$	<table><tr><td>C_7H_{11}</td><td>$\frac{He^*}{1}$</td><td>$\frac{H_2^*}{2}$</td></tr><tr><td>C_6H_7O</td><td>$\ddot{1}$</td><td>$\ddot{1}$</td></tr></table>	C_7H_{11}	$\frac{He^*}{1}$	$\frac{H_2^*}{2}$	C_6H_7O	$\ddot{1}$	$\ddot{1}$	<table><tr><td>C_7H_{11}</td><td>$\frac{He^*}{2}$</td><td>$\frac{H_2^*}{1}$</td></tr><tr><td>C_6H_7O</td><td>$\ddot{3}$</td><td>$\ddot{1}$</td></tr></table>	C_7H_{11}	$\frac{He^*}{2}$	$\frac{H_2^*}{1}$	C_6H_7O	$\ddot{3}$	$\ddot{1}$
C_7H_{11}	$\frac{He^*}{3}$	$\frac{H_2^*}{2}$																										
C_6H_7O	$\ddot{2}$	$\ddot{1}$																										
C_7H_{11}	$\frac{He^*}{1}$	$\frac{H_2^*}{1}$																										
C_6H_7O	$\ddot{1}$	$\ddot{1}$																										
C_7H_{11}	$\frac{He^*}{1}$	$\frac{H_2^*}{2}$																										
C_6H_7O	$\ddot{1}$	$\ddot{1}$																										
C_7H_{11}	$\frac{He^*}{2}$	$\frac{H_2^*}{1}$																										
C_6H_7O	$\ddot{3}$	$\ddot{1}$																										
91	C_7H_7	C_7H_7	C_7H_7	—																								
80	C_6H_8	C_6H_8	C_6H_8	C_6H_8																								
79	C_6H_7	—	C_6H_7	—																								
78	C_6H_6	C_6H_6	C_6H_6	C_6H_6																								
70	C_4H_6O	C_4H_6O	C_4H_6O	C_4H_6O																								
68	C_5H_8	C_5H_8	C_5H_8	C_5H_8																								
67	C_5H_7	—	C_5H_7	—																								
57	C_3H_5O	C_3H_5O	C_3H_5O	C_3H_5O																								

* See text for explanation.

TABLE V

High Resolution Results for Tricyclic Alcohols



<u>m/e</u>		<u>m/e</u>		
112	C ₇ H ₁₂ O	110	C ₇ H ₁₀ O	
94	C ₇ H ₁₀	95	C ₆ H ₇ O	
81	C ₆ H ₉	92	C ₇ H ₈	
79	C ₆ H ₇	91	C ₇ H ₇	
			He* H ₂ *	

70	C ₄ H ₆ O	82	C ₅ H ₆ O	4 1
			
68	C ₅ H ₈		C ₆ H ₁₀ 1 1	
			He* H ₂ *	

57	C ₃ H ₅ O	81	C ₅ H ₅ O	1 Trace
			
			C ₆ H ₉ 5 1	
		79	C ₆ H ₇	
		78	C ₆ H ₆	
		67	C ₅ H ₇	

TABLE VI

High Resolution Results for Bicyclic Alcohols

* See Text for explanation

and probable structure for the ion. While a knowledge of the elemental composition of the fragments aids in the interpretation of the mass spectra no unequivocal decision can be made as to which atoms originally present in the molecule are retained by the particular fragment.

Probable fragmentation schemes together with probable structures for the major fragments of the compounds studied are shown in figures 15-21. Although only one isomer of a group is shown, the proposed scheme is applicable to all isomers of the group. For many fragments more than one pathway exists for the formation of that fragment. Also since isotopic substitution was not used, it cannot be stated unequivocally that the proposed pathway actually exists.

G. Ionization Potentials

Electron impact ionization potentials were obtained for all compounds used in this study by use of a method similar to that described by Lossing et al (59), the results obtained are shown in figure 22. Previous work in this laboratory, using the same technique, has shown that the reproducibility is about ± 0.1 e.V. The values obtained show that the ionization potential of the exo isomer is greater than that of the corresponding endo isomer in all instances. The release of non-bonded interaction energy in the more crowded endo isomer may be used to account for the lower ionization potentials of the endo isomer compared to the corresponding exo isomer.

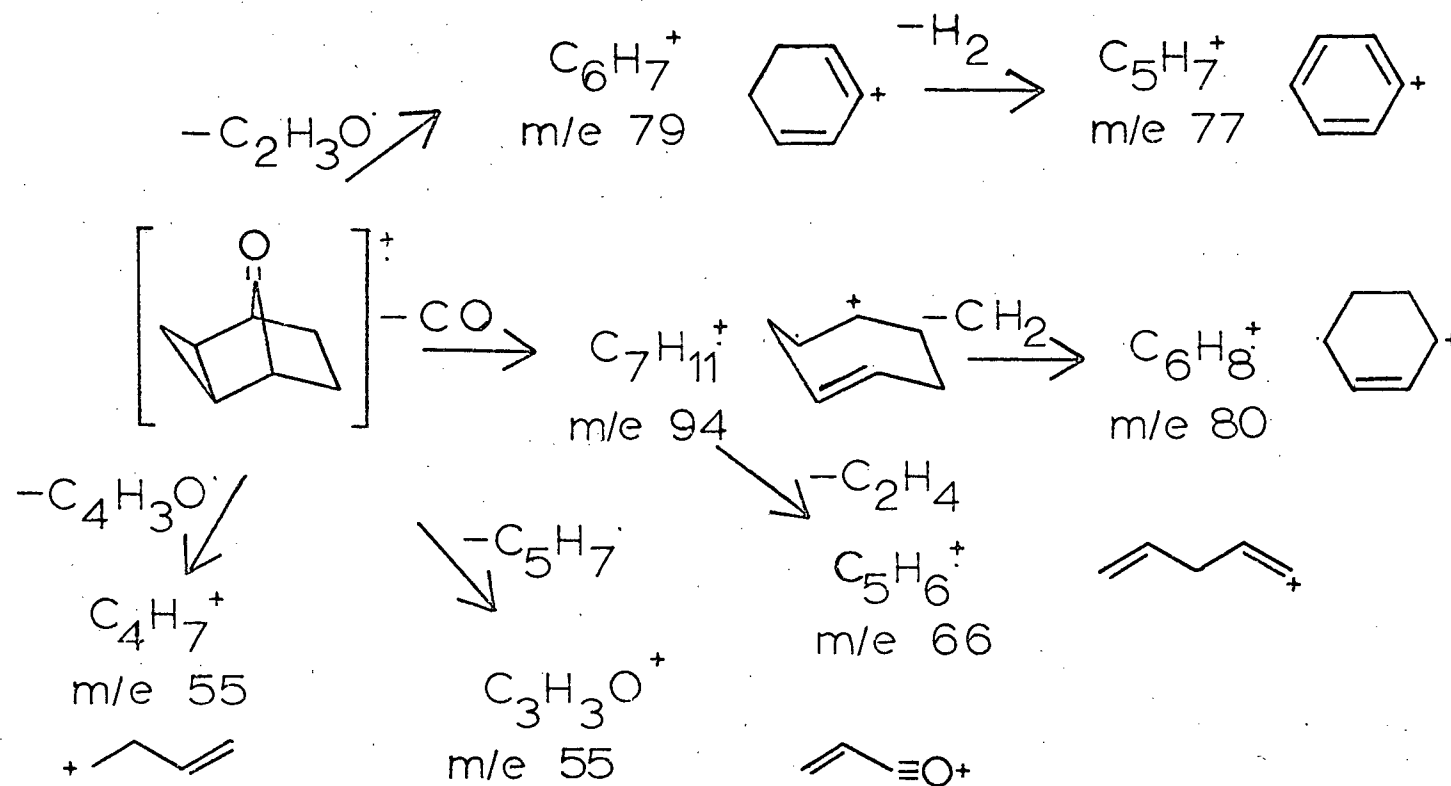


Figure 15. Fragmentation Scheme for Tricyclic Ketones.

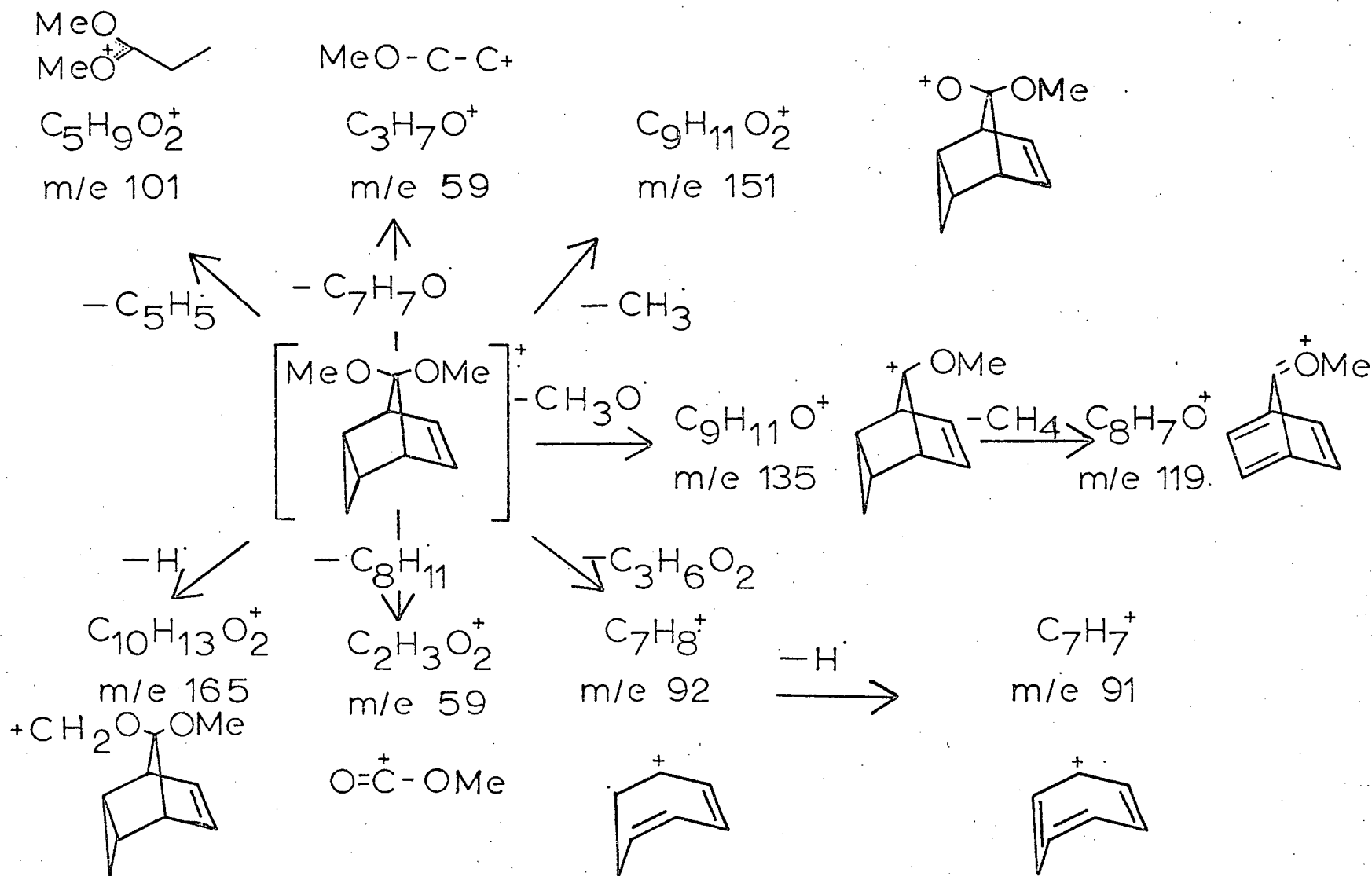


Figure 16. Fragmentation Scheme for Unsaturated Tricyclic Methoxy Compound.

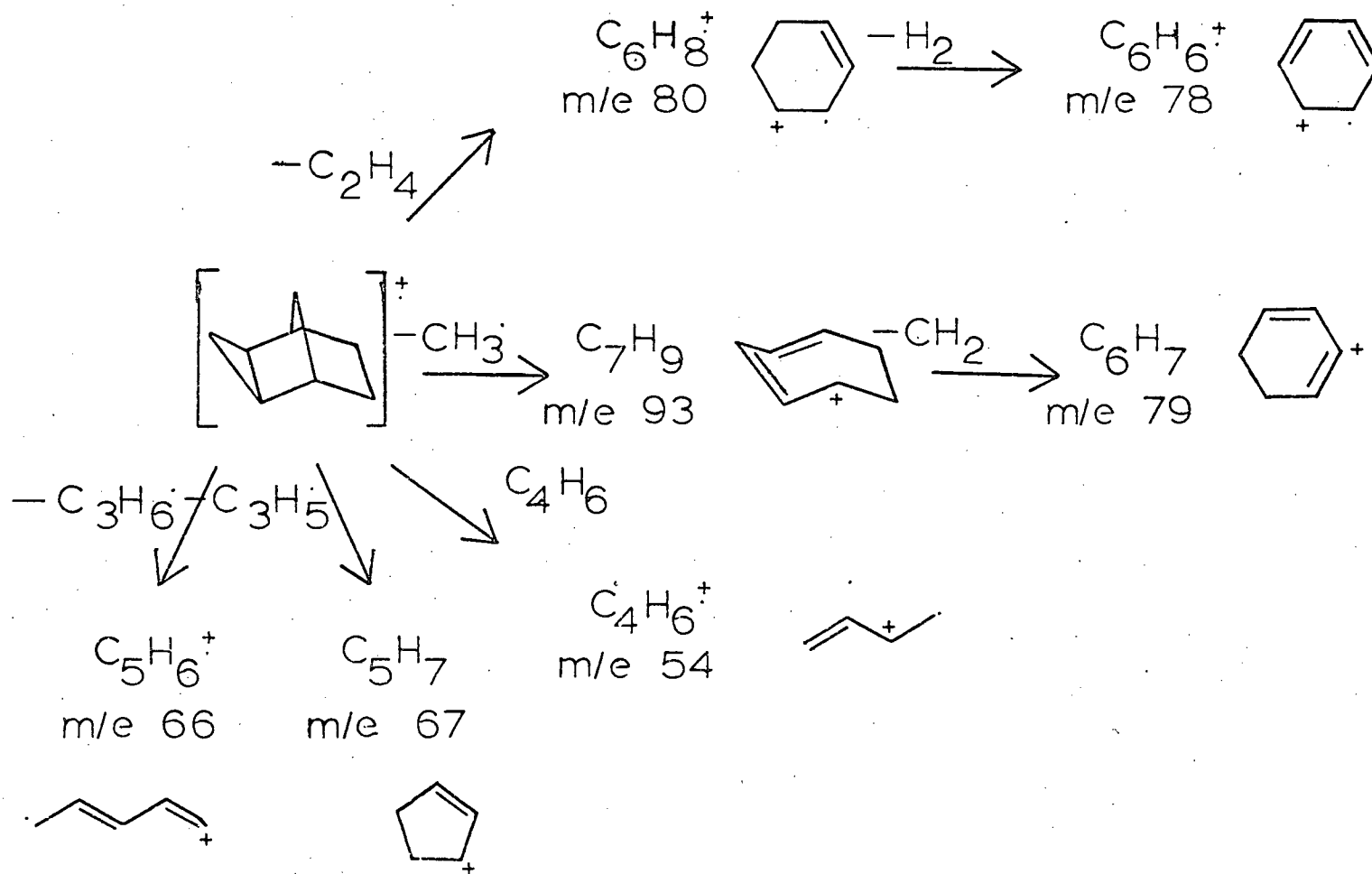


Figure 17. Fragmentation Scheme for Tricyclic Hydrocarbons.

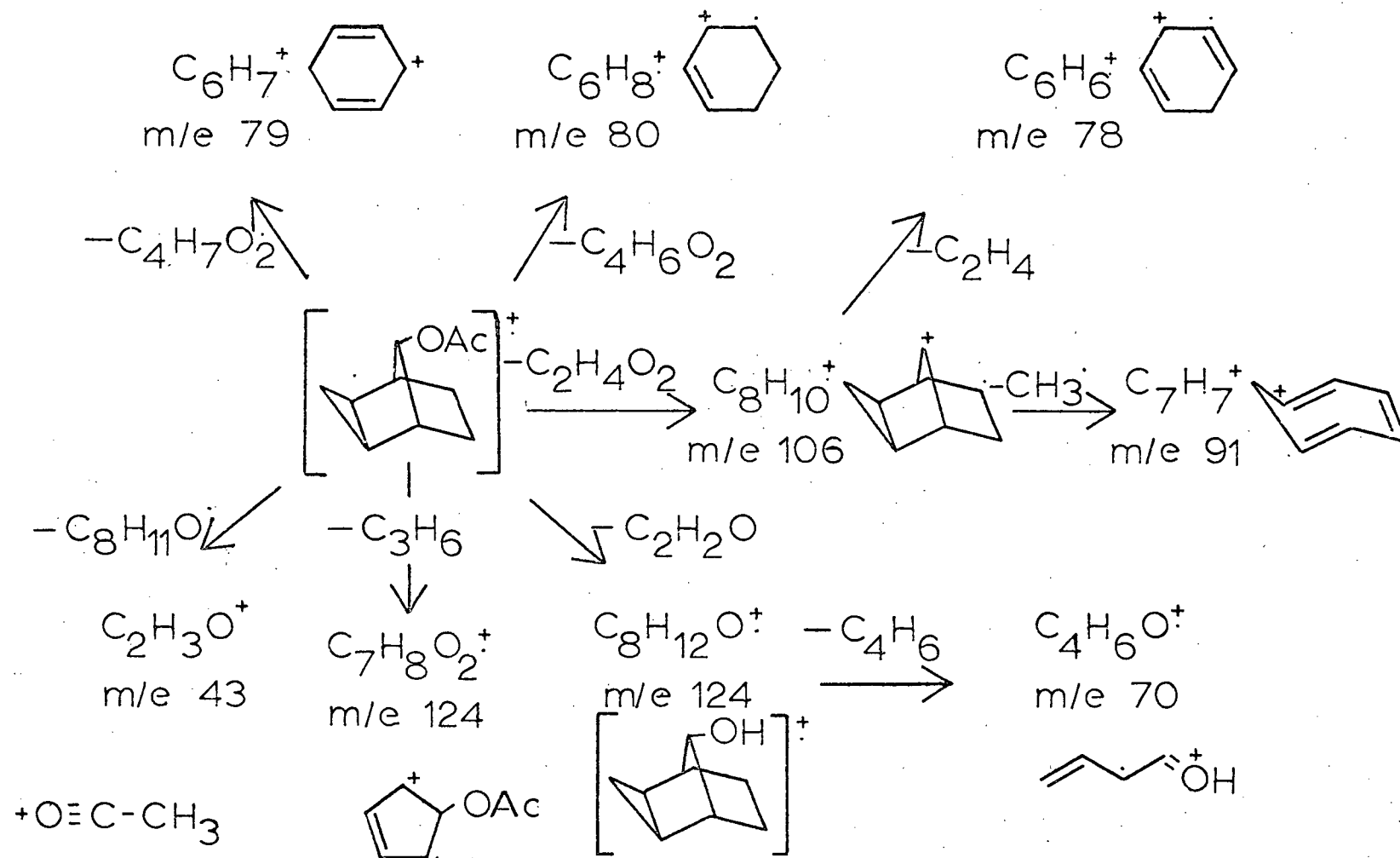


Figure 18. Fragmentation Scheme for Tricyclic Acetates.

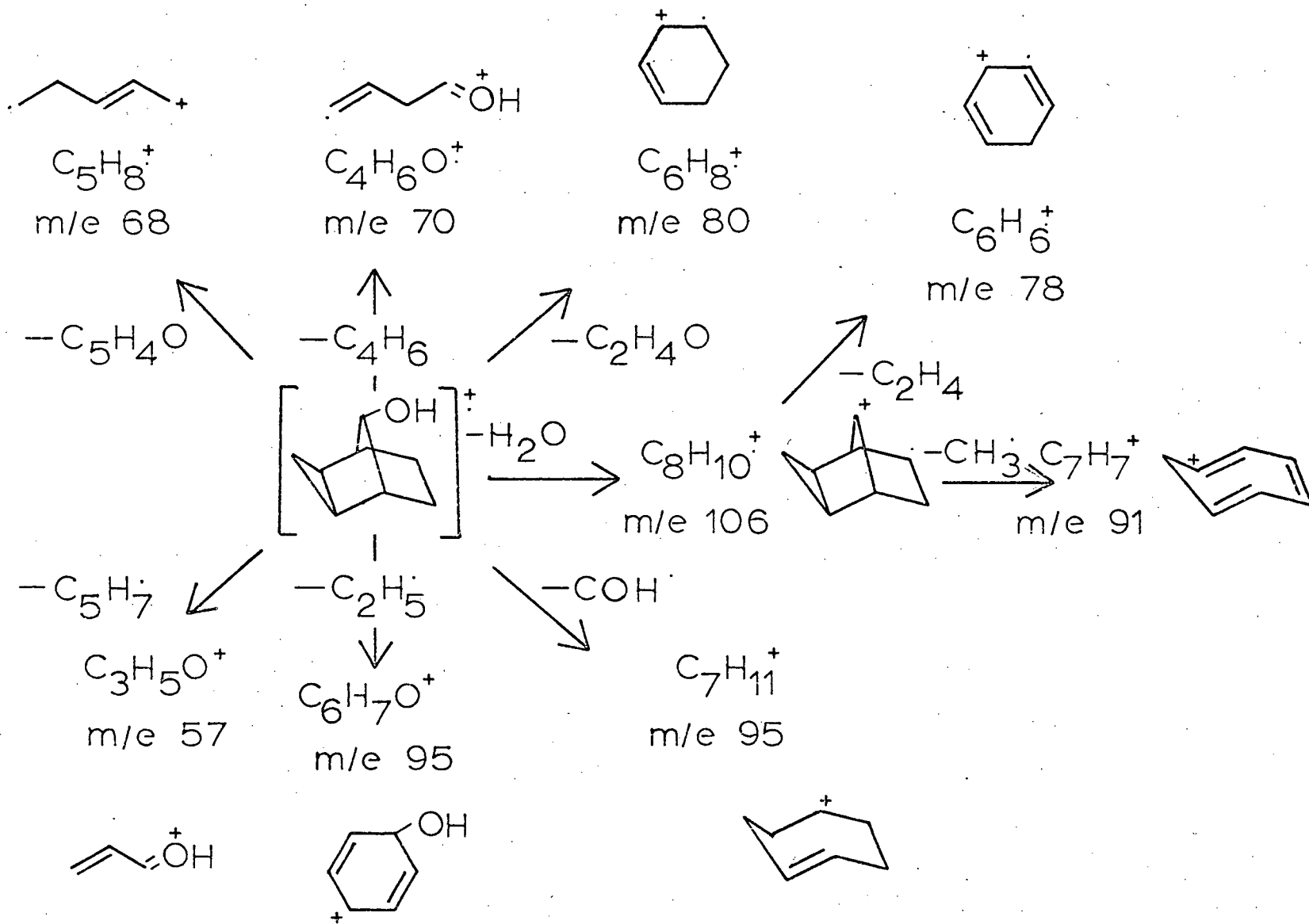


Figure 19. Fragmentation Scheme for Tricyclic Alcohols.

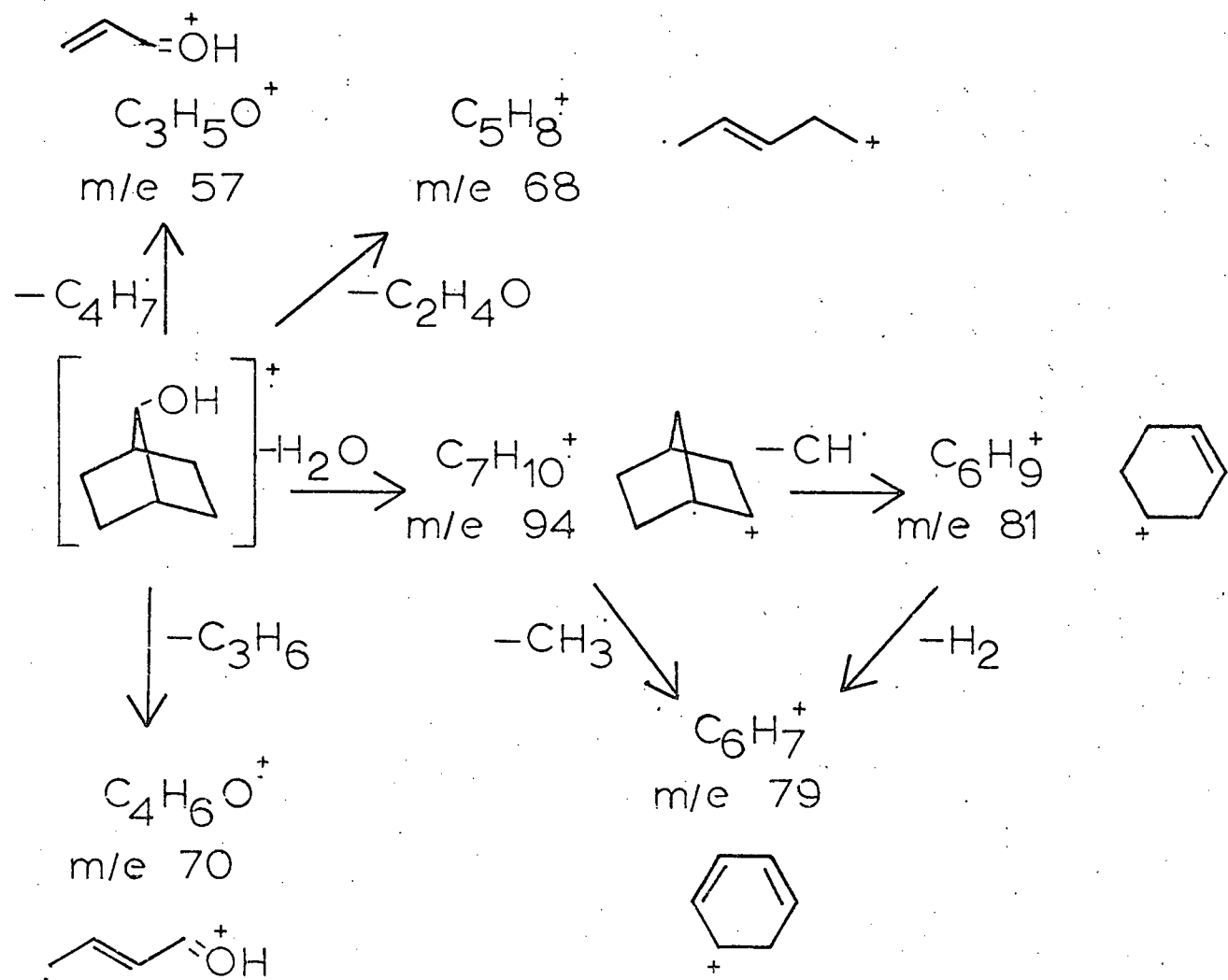


Figure 20. Fragmentation Scheme for Bicyclo [2.2.1] heptan-7-ol

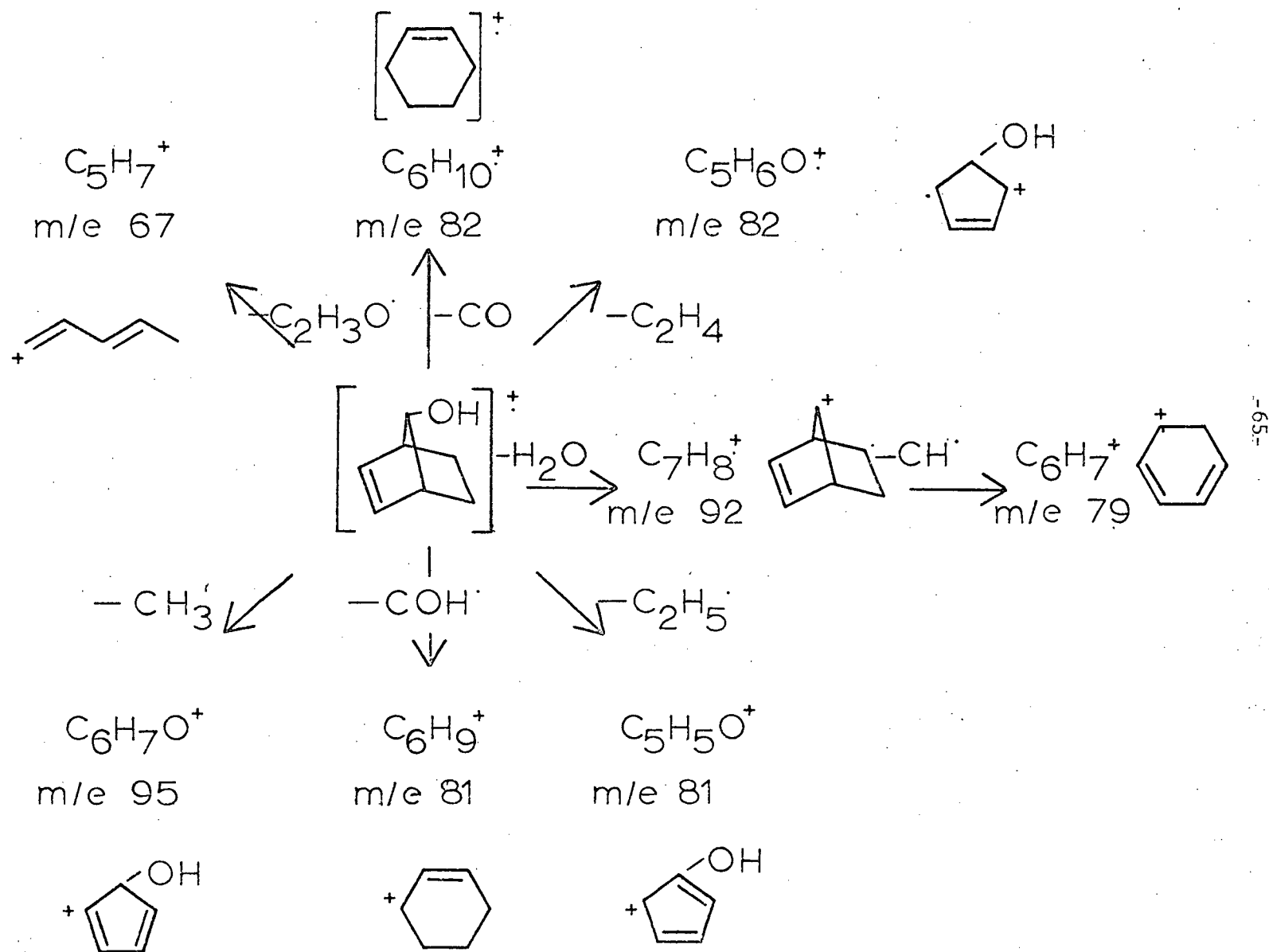


Figure 21. Fragmentation Scheme for anti-bicyclo [2.2.1] hepten-7-ol.

It can also be seen from figure 22 that for the cases studied the ionization potential of the unsaturated compounds are less than that of the corresponding saturated ones as is expected (64). The reduction in ionization potential may be attributed to the delocalization effect of the pi system which results in the electrons being less tightly bound. Also from figure 22 it can be seen that the ionization potential of the anti isomer is greater than that of the corresponding syn isomer. No reason has been found to account for the phenomenon.

Natalis (5) has found from thermodynamic data that cis isomers are generally less stable than the corresponding trans isomer, the energy difference being a measure of the interaction energy arising from the steric conformation. Also since the cis isomer is less stable, fragmentation occurs more readily. The effect that the more sterically hindered (less stable) isomer fragments more readily also appears to be present in the isomers studied.

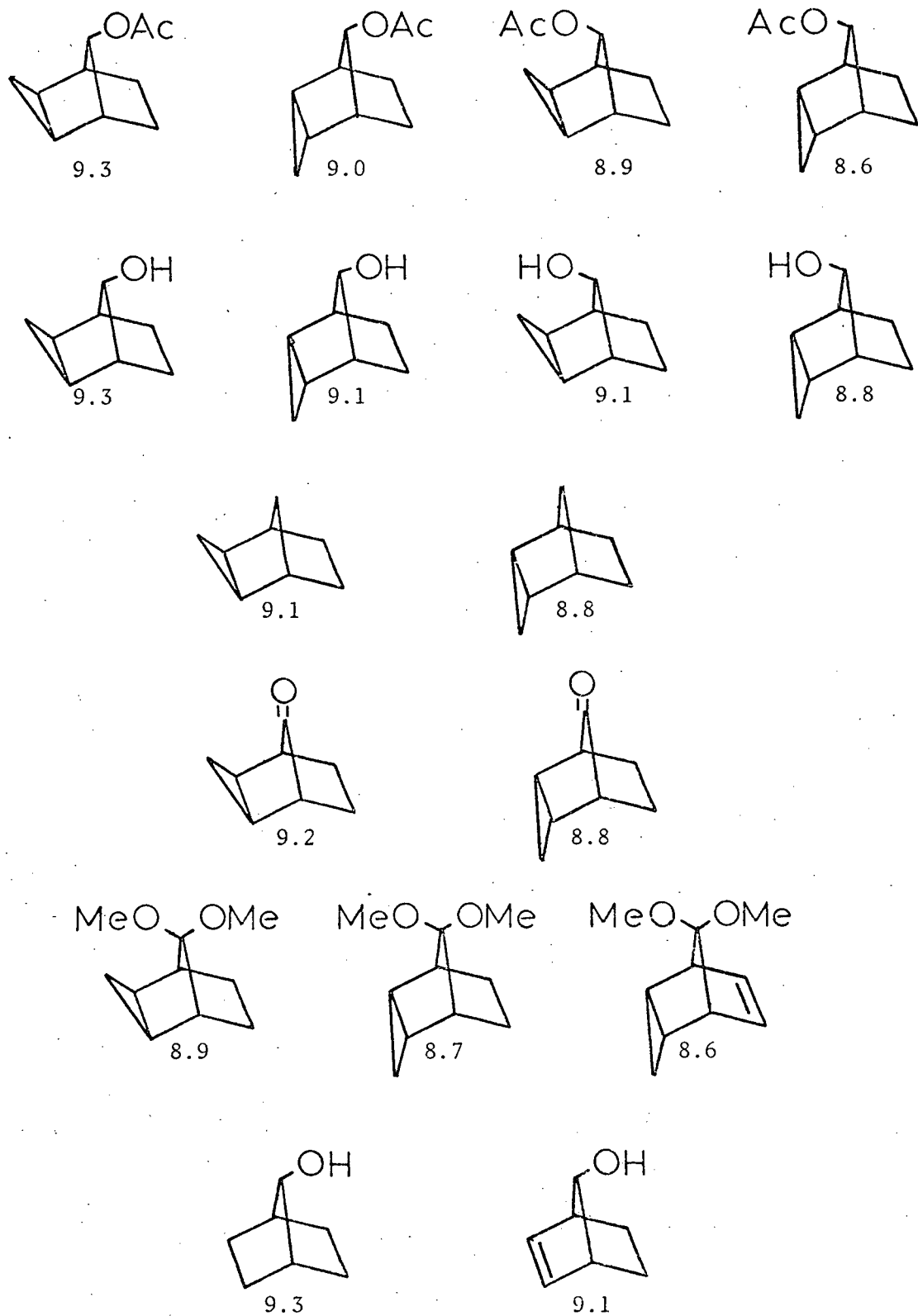


Figure 22. Ionization Potentials for Compounds Studied (in e.v.).

V CONCLUSION

The mass spectra for the isomers of a group are qualitatively very similar. However, significant differences are observed in the relative abundances of the principal fragments. The observed differences are more pronounced when the hydrogen light source is used than when the helium light source is used, however, with the hydrogen light source fewer differences are observed.

The facility of fragmentation appears to be a function of steric hindrance within the molecule. Thus the endo isomers fragment more readily than do the exo ones except for the exo-syn acetate in which a large 'bowsprit-flagpole' interaction is present. This occurs because the exo compounds have a fixed boat like conformation in which steric interaction may occur between the cyclopropyl ring and any large group on the syn 'flagpole' position. For the compounds studied the more crowded (i.e. the larger the substituent on the 'flagpole' position) the isomer, the smaller the relative abundance of the molecular ion.

The probable formation of a seven membered ring appears to occur more readily for endo isomers than for the corresponding exo isomer because in the endo isomers the orbitals forming the cyclopropyl 'banana' bond are ideally situated for interaction and subsequent pi bond formation with the p type orbitals available on fragmentation. Thus fragments which probably involve a seven membered ring as an intermediate are more intense for the endo isomer than the corresponding exo isomer.

The ionization potential of the endo isomer is lower than that of the corresponding exo isomer. The release of non-bonded interaction energy in crowded molecules is presumably the reason for the lower ionization potential.

Because the mass spectra of isomers are qualitatively very similar it appears that the use of photoionization mass spectrometry will only be slightly more useful than electron impact mass spectrometry for the identification of geometrical isomers. Using photoionization it will be necessary to have previously determined the mass spectra of all isomers of a group before any particular isomer can be identified.

VI BIBLIOGRAPHY

1. K. Biemann, "Mass Spectrometry", McGraw-Hill, New York (1962).
2. H. Mandelbaum and D. Ginsberg, Tetra. Letters, 2479 (1965).
3. J.E. Gurst and C. Djerrassi, J. Am. Chem. Soc., 86, 5542 (1964).
4. M. Fetizon in "Some Newer Physical Methods in Structural Chemistry", ed. R. Bonnett and J.G. Davis, United Trade Press, Ltd., London (1967).
5. P. Natalis in "Mass Spectrometry" ed. R.I. Reed, Academic Press, New York (1965).
6. P. Natalis, Bull. Soc. Chim. Belg., 66, 5 (1957).
7. J. Momigny and P. Natalis, ibid., 66, 26 (1957).
8. P. Natalis, ibid., 69, 519 (1960).
9. P. Natalis, Nature, 197, 73 (1963).
10. P. Natalis, Bull. Soc. Chim. Belg., 72, 264 (1963).
11. P. Natalis, ibid., 72, 374 (1963).
12. P. Natalis, ibid., 72, 416 (1963).
13. P. Natalis and J. Laune, ibid., 73, 944 (1964).
14. P. Natalis, ibid., 73, 961 (1964).
15. P. Natalis and J.L. Franklin, ibid., 75, 328 (1966).
16. P. Natalis, ibid., 75, 668 (1966).
17. R. Elliott ed., "Advances in Mass Spectrometry", vol. 2, Pergamon Press, Oxford (1962).
18. C.E. Brion and L.D. Hall, J. Am. Chem. Soc., 88, 3661 (1966).
19. C.E. Brion, Anal. Chem., 37, 1706 (1965).
20. C.E. Brion, ibid., 38, 1941 (1966).
21. W.P. Poschenrieder and P. Warneck, ibid., 40, 385 (1968).
22. W.P. Poschenrieder and P. Warneck, J. Appl. Phys., 37, 2812 (1966).
23. A. Terenin and B. Popov, Physik Z. Sowjetunion, 2, 299 (1932).

24. N. Wainfan, W.C. Walker and G.L. Weissler, J. Appl. Phys., 24, 1318 (1957).
25. K. Watanabe, F.F. Marmo and E.C.Y. Inn, Phys. Rev. 91, 1155 (1953).
26. F.P. Lossing and I. Tanaka, J. Chem. Phys., 25, 1031 (1956).
27. A.N. Terenin and G. Vilessov in "Advances in Photochemistry", vol. 2, ed. W.A. Noyes, Interscience Pub., New York (1964).
28. H. Hurzeler, M.G. Inghram and J.D. Morrison, J. Chem. Phys., 27, 313 (1957).
29. J.D. Morrison, H. Hurzeler, M.G. Inghram and H.E. Stanton, J. Chem. Phys., 33, 821 (1960).
30. G.L. Weissler, J.A.R. Samson, M. Ogawa and R.G. Cook, J. Opt. Soc. Am., 49, 338 (1959).
31. F.J. Comes and W. Lessmann, Z. Naturforsch., 19a, 1230 (1964).
32. M. Al-Joboury and D.W. Turner, J. Chem. Soc., 5141 (1963).
33. D.C. Frost, C.A. McDowell and D.A. Vroom, Proc. Roy. Soc., A296, 566 (1967).
34. D.C. Frost, D. Mak and C.A. McDowell, Can. J. Chem., 40, 1064 (1962).
35. V.H. Dibeler and R.M. Reese, J. Chem. Phys., 40, 2034 (1964).
36. J. Berkowitz and W.A. Chupka, J. Chem. Phys., 45, 1287 (1966).
37. I. Omura and H. Doi, Japan J. Appl. Phys., 6, 275 (1967).
38. I. Omura and H. Doi, Bull. Chem. Soc. Japan, 40, 1090 (1967).
39. I. Omura and H. Doi, Japan J. Appl. Phys., 6, 116 (1967).
40. J.H. Beynon, A.E. Fontaine, D.W. Turner and R.E. Williams, J. Sci. Inst., 44, 283 (1967).
41. C.E. Brion and G.E. Thomas, J. Mass. Spec. and Ion. Phys., 1, 25 (1968).
42. S. Geltman, Phys. Rev., 102, 171 (1956).
43. C.A. McDowell ed., "Mass Spectrometry", McGraw-Hill, New York (1963).
44. J. Franck, Trans. Far. Soc., 21, 536 (1925).
45. E.V. Condon, Phys. Rev. 32, 858 (1928).

46. F.H. Field and J.C. Franklin, "Electron Impact Phenomena", Academic Press, New York (1957).
47. H.W. Massey and E.H. Burhop, "Electronic and Ionic Impact Phenomena", Oxford University Press (1952).
48. G.P. Barnard, "Modern Mass Spectrometry", Institute of Physics London, (1953).
49. G.P. Barnard, "Mass Spectrometry Researches", N.P.L., H.M.S.O. (1956).
50. J.H. Beynon, "Mass Spectrometry and Its Applications to Organic Chemistry", Elsevier, Amsterdam (1960).
51. R.P. Craig, B.N. Green and J. D. Waldron, *Chimia*, 17, 33 (1963).
52. C.E. Brion, Unpublished results.
53. C.E. Brion and W.B. Stewart, *Nature*, 217, 946 (1968).
54. D.C. Frost and C.A. McDowell, Air Force Cambridge Research Laboratory Document, # TR-60-423 (1960).
55. G. Herzberg, "Atomic Spectra and Atomic Structure", Second Edition, Dover Publications, New York (1964).
56. M. Zelikoff, P.H. Wychoff, C.M. Auschenbrand and R.S. Loomis, *J. Opt. Soc. Am.*, 49, 338 (1952).
57. J.A.R. Samson, "Techniques of Vacuum Ultraviolet Spectroscopy", J. Wiley and Sons, New York, (1967).
58. J.S. Haywood-Farmer, Ph.D. Thesis, University of British Columbia (1967).
59. F.P. Lossing, A.W. Tickner and W.A. Bryce, *J. Chem. Phys.*, 19, 1254 (1951).
60. B. Halton, M.A. Battiste, R. Rehberg, C.L. Deyrup and M.E. Brennan, *J. Am. Chem. Soc.*, 89, 5964 (1967).
61. H. Tanida, T. Tsuji and T. Irie, *J. Am. Chem. Soc.*, 89, 1953 (1967).
62. S.C. Clarke and B.L. Johnson, *Tetrahedron Letters*, 617 (1967).
63. H. Budzikiewicz, C. Djerassi and D.H. Williams, "Mass Spectrometry of Organic Compounds", Holden Day, Inc., San Francisco (1967).
64. R.I. Reed, "Applications of Mass Spectrometry to Organic Chemistry", Academic Press, London (1966).